THE UNIVERSITY OF ALBERTA

RELEASE FORM

NAME OF AUTHOR: Richard Anthony Reynolds

TITLE OF THESIS: Positron Tomography with Multiwire Proportional Chambers

DEGREE FOR WHICH THESIS WAS PRESENTED: Master of Science

YEAR THIS DEGREE GRANTED: 1973

THE UNIVERSITY OF ALBERTA

# POSITRON TOMOGRAPHY
# WITH MULTIWIRE PROPORTIONAL CHAMBERS

by

© RICHARD ANTHONY REYNOLDS

A THESIS

SUBMITTED TO THE FACULTY OF GRADUATE STUDIES AND RESEARCH

IN PARTIAL FULFILMENT OF THE REQUIREMENTS FOR THE DEGREE

OF MASTER OF SCIENCE

IN

BIOPHYSICS

DEPARTMENT OF PHYSICS

EDMONTON, ALBERTA

FALL, 1973

THE UNIVERSITY OF ALBERTA

FACULTY OF GRADUATE STUDIES AND RESEARCH

The undersigned certify that they have read, and recommend to the faculty of Graduate Studies and Research, for acceptance, a thesis entitled POSITRON IMAGING WITH MULTIWIRE PROPORTIONAL CHAMBERS submitted by Richard Anthony Reynolds in partial fulfilment of the requirements for the degree of Master of Science in Biophysics.

# DEDICATION

For Mr. F. A. L. Gardner, my teacher

# ABSTRACT

A new gamma camera in which multiwire proportional chambers (MWPCs) are used as position-sensitive detectors to obtain tomographic images of a distribution of positron emitting radionucleides is described. The theoretical performance of such an instrument is discussed, and compared to existing positron gamma cameras. The properties and applications of multiwire proportional chambers are reviewed, and the design and construction of a prototype MWPC positron camera is described in detail. Some images obtained with the camera are presented, the camera is evaluated, and modifications incorporating recent work in other laboratories are suggested.

ACKNOWLEDGEMENTS

I wish to thank my supervisor, Dr. R. E. Snyder, who initiated this project, and gave generously of his time in overseeing my work and in the preparation of this thesis; and Dr. T. R. Overton, who made it possible for me to work in a Medical Physics environment, and who has taught me much, both through example and through his off-the-cuff advice and suggestions. Their help is sincerely appreciated.

I wish to thank also the staff of the Lawrence Radiation Laboratory, Berkeley, and in particular Dr. Leon Kaufman, who made much unpublished material available, and kindly supplied us with circuit diagrams on which the following are based: Preamplifiers, Constant Fraction of Pulse Height Triggers, and Time-to-Amplitude Converters.

My greatest single debt must be to Len Friedenberg, who has drawn from his expertise in Biomedical Engineering to give me advice and practical help on every conceivable aspect of this project. I am indebted also to Gordon Blinston for many helpful discussions on programming, and for permission to use his subroutines DOSTP and DCODE; and to Mike Marriott who gave me help with some aspects of the computer system.

I wish to thank also Mr. Nick Riebeck for his helpful advice and Mr. Walter Volk for his meticulous machine work in constructing the wire chambers; and Mr. Ernie Pearce who gave me much patient advice and assistance with the

construction of the wire planes.

Finally I wish to express my sincere appreciation to Fedos and Ingrid Panayi for their friendship, help and encouragement thrcughout my stay in Edmonton, and to my wife Shirley, whc tcok the phctcgraphs and formatted the manuscript for computer.

TABLE OF CONTENTS

## LIST OF ILLUSTRATIONS

# CHAPTER 1

## INTRODUCTION

Although medical physics is not a new field, the area of nuclear medicine has exhibited rapid growth in recent years, particularly following the proliferation of nuclear reactors and the increased availability of radioisotopes. One important aspect of nuclear medicine is the development of techniques for imaging normal or abnormal organs - for example, radioisotope imaging has become the accepted method of diagnosing and localising brain tumours (Brownell and Shalek 1970) - and it is with an imaging device that this thesis is concerned.

The basic problem in radioisotope imaging is to deduce the volume distribution of a radioisotope within an organ from the pattern of radiation leaving the surface of the body, and to display this information in an easily interpreted form (Mallard 1967). In general, this requires three pieces of apparatus: a radiation detector, a display system, and a collimator or other method of producing a mapping between object and detector. In addition, one must determine both the intensity of radiation reaching the detector, and the point in space at which the detector intercepts it. This is most easily accomplished by physically moving a detector with a small field of view in a raster-like pattern, recording the intensity of radiation at

each of a number of points. Historically, such "scanners" were the first imaging systems to be employed. Although superseded by "gamma cameras" for some applications, rectilinear radioisotope scanners retain the advantage that with a focused collimator, only one plane of the object will be in sharp focus throughout the scan.

The gamma camera, as developed by Anger (1958), employs a stationary position-sensitive detector to view all parts of the isotope distribution simultaneously instead of scanning it point by point. The rate of data acquisition is not limited by mechanical factors and thus the same information can be gathered in a much shorter time than with a scanner. Rapid sequences of images can be used to study dynamically the behaviour of an organ over a short period of time, or different static views of the same organ can be taken within a short period of time.

The position-sensitive detector used in the Anger camera is a single large thallium-activated sodium-iodide crystal. The position of a scintillation is deduced electronically by comparing the outputs of nineteen photomultiplier tubes. More recently, systems based on many other position-sensitive detectors have been devised. Of note are the use of intensifying image orthicons (Ter-Pogossian, Kastner and Vest 1963), solid state detectors (McCready, Parker, Gunnersen, Ellis, Moss, Gore and Bell 1971), spark chambers (Kellershohn, Desgrez and Lansiart

1964), and multiwire proportional chambers (Kaufman, Perez-Mendez, Shames and Stoker 1972). These multiwire proportional chambers (MWPCs) combine good spatial resolution (1 mm), high count rates ($10^6$ per second) and good uniformity with large area, ease of construction and low cost. However, due to their low sensitivity to high energy gamma rays, these devices have been mostly used with low energy isotopes such as $^{125}I$ or $^{133}Xe$. In this respect, they have been complementary to the Anger camera which is most useful for energies above 100 keV.

A second area in which MWPCs may be useful is in the detection of annihilation radiation from tissue labeled with a positron-emitting radioisotope. Such radioisotopes afford a number of advantages, to be described in a later chapter: in particular, by using two detectors, an expensive, massive and inefficient collimator can be avoided. Recent results (Lim, Chu, Kaufman, Perez-Mendez and Sperinde 1973) indicate that by using suitably shaped lead foils to convert the annihilation radiation to electrons, MWPCs with efficiencies approaching 8% can be constructed.

This thesis describes a prototype positron camera which uses multiwire proportional chambers. A laboratory digital computer system is used to acquire, analyse and display the data from the camera. The theoretical performance of such a camera is discussed and compared to other positron camera systems currently available. Results

obtained from the prototype system show that the approach is viable, and that with the improvements to the design indicated in the final chapter, a practical MWPC positron camera can be realized.

# CHAPTER 2

# POSITRON IMAGING WITH MULTIWIRE PROPORTIONAL CHAMBERS

## 2.1 Tomography and Positron Imaging.

A basic problem with diagnostic radiology is that an organ of interest may be hidden behind an overlying structure of bone. The organ will be particularly hard to visualize with x-rays, because the difference in absorption between bone and tissue is more pronounced at lower energies. One long established solution (Zeides des Plantes 1932) is illustrated in Figure 1: the x-ray tube and the film are moved parallel to each other but in opposite directions so that one plane of the patient's body casts its shadow on the same part of the film throughout. This plane will be in focus, while planes above and below it will be blurred by the movement. The effect obtained is that of a cross-section through the body. This technique, called tomography, has been borrowed by nuclear medicine, where it is used mostly to obtain this cross-section effect when imaging large organs. For example, a tumour may be located by examining different planes of the body until it appears in sharpest focus.

A number of gamma cameras which work in a manner analogous to the x-ray equipment have been devised. These employ rotating collimators with slanted holes. In one system (Kuhl 1967), electronic compensation is made for this

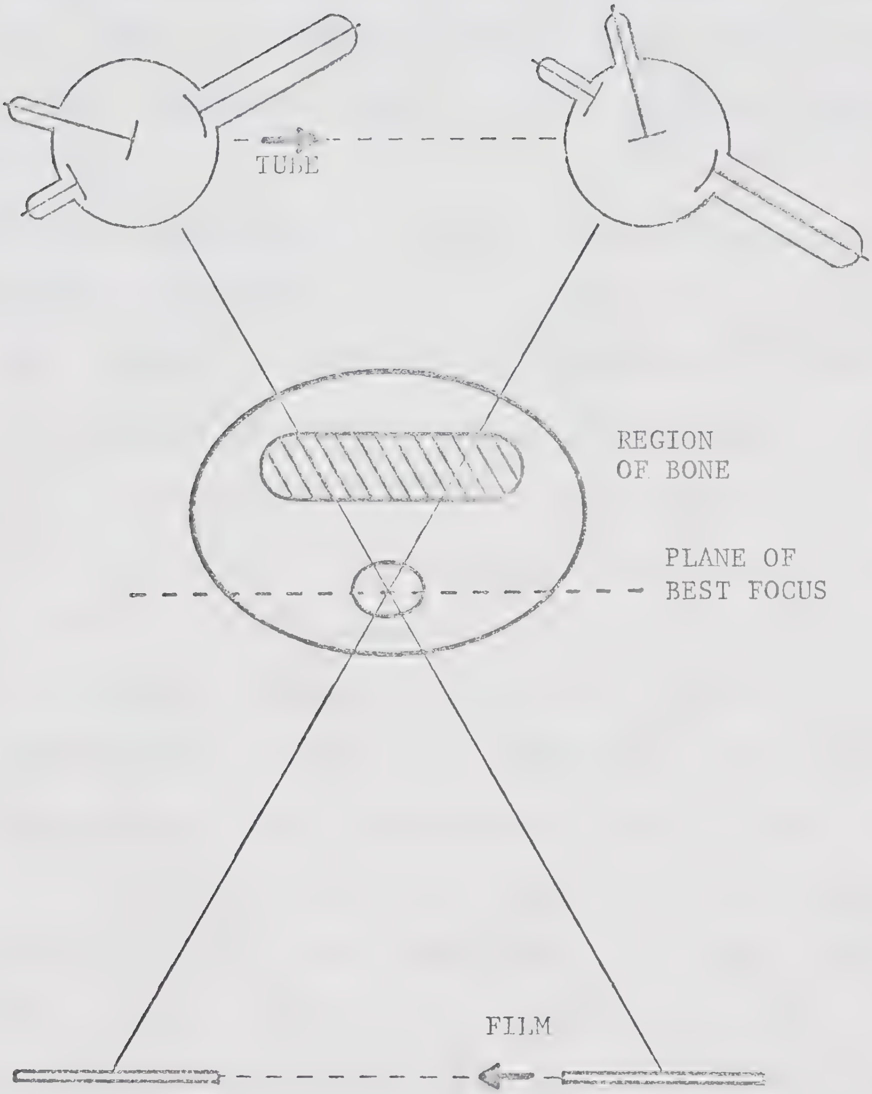


Figure 1: Principle of X-ray Tomography

rotation in the plane of interest only: in other planes, point sources are blurred out into small circles. In another system (Freedman 1970), the collimator stops and images are taken at twelve positions 30° apart; a digital computer then combines these twelve images into one tomographic view.

Positrons emitted by proton-rich nuclei can also be used to produce tomographic images (Wrenn, Good and Handler 1951). In tissue, a positron emitted with an energy of 1 MeV will be thermalized within 4 mm, and will be captured by an electron to form positronium. In the majority of cases, positronium will decay to form two 511 keV gamma rays, and since it is almost at rest, these will emerge along the same straight line but in opposite directions (Figure 2). By using two position sensitive detectors, the "position vector" along which the annihilation took place can be deduced. By measuring the time taken by each gamma ray to reach its detector, one can determine at what depth the annihilation took place, and produce a truly three-dimensional image. This time-of-flight technique requires very high speed timing for good spatial resolution, but with the techniques then available, resolutions of 15 cm were reported by Burnham, Aronow and Brownell in 1967. A simpler technique is to choose a likely "plane of best focus", and calculate the intersections of all position vectors with this plane. Objects actually located in this plane will form a sharp image; objects in other planes become blurred

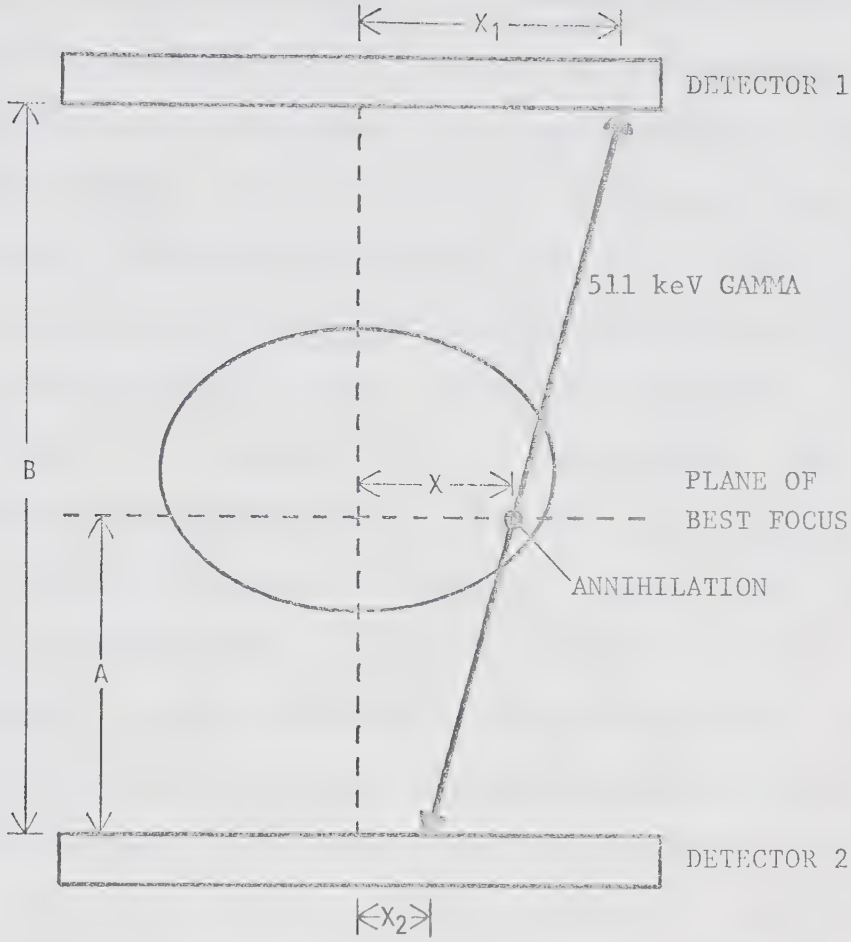


$$\boxed{X = X_2 + \frac{A}{B}(X_1 - X_2)}$$

Figure 2: Principle of Positron Tomography

and form part of the background. A tomographic image rather than a truly three-dimensional image is formed, but the depth resolution is better and the instrumentation required is much less complex. This approach has been used by Anger and Rosenthal (1959) to develope a positron version of the Anger gamma camera; positron-imaging scanners have also been developed by Brownell and Sweet (1953), and others.

Apart from the possibilities of tomography, there are other advantages in using positron-emitters for radioisotope imaging. The two detectors completely specify the position vector of the annihilation, and no collimator is necessary. The high energy of the annihilation radiation is well suited to imaging deep lying organs. Attenuation of the radiation is a function only of the total thickness of tissue traversed and not of the depth of the organ; as a consequence, activities can be determined absolutely (Burnham, Aronow and Brownell 1967). Some medically important elements - such as carbon, oxygen and nitrogen - have positron emitting isotopes but no suitable gamma emitting isotopes. Finally, many positron emitters are short lived isotopes with a high specific activity. Thus a high initial activity can be administered for rapid imaging, but the total dose to the patient will be small.

## 2.2 The Possibilities of MWPCs.

While the Anger positron camera has been widely and

successfully employed, it has certain limitations. We believe that by using multiwire proportional chambers as position-sensitive detectors, a less expensive system offering better spatial resolution, a larger field of view, and comparable statistics can be realized. To substantiate these claims, we estimate below the typical count rate, the efficiency and the sensitivity of a positron camera based on MWPCs.

For a radiation detector of efficiency e and geometric factor G, the count rate is

$$R = GeN \tag{1}$$

where N is the rate at which radiation leaves the body under observation. If a point source of positrons is placed midway along the common axis of two similar detectors facing each other, the rate at which annihilation radiation is detected coincidentally by both detectors is

$$C = 2Ge^2N \tag{2}$$

where N is now the rate of annihilation of positrons. The maximum useful rate of annihilation is limited by the maximum background that can be tolerated. Assuming the isotope emits one positron and no gamma rays per disintegration, the principal background will be caused by two (or more) distinct disintegrations occurring within the coincidence resolving time of the system. Background due to radiation from other sources will be negligible. If the

resolving time is t, the number of accidental coincidences occurring per second is

$$A = 8G^2e^2N^2t. \qquad (3)$$

If a background of 10% can be tolerated, we have

$$A/C = 4GNt \leq 0.1 \qquad (4)$$

and therefore

$$N \leq 0.1/4Gt. \qquad (5)$$

For two wire chambers each of area 25 cm square placed 25 cm apart, G = 1/6; the coincidence resolving time is limited by the time resolution of the wire chambers, which is typically 30 nsec (Cunitz, Sippach and Dieperink 1971; Grunberg, Cohen and Mathieu 1970); thus the maximum useful source strength is

$$N = 5 \times 10^6 \text{ dis/sec} = 0.14 \text{ mCi}. \qquad (6)$$

This compares favorably with the Anger positron camera, for which maximum source strengths of between 25 microcuries (Nuclear Chicago Corporation 1967) and 150 microcuries (Monahan, Beattie and Laughlin 1972) are recommended.

Recent reports (Lim, Chu, Kaufman, Perez-Mendez and Sperinde 1973) indicate that through the use of shaped converter foils, MWPCs with efficiencies of up to 8% for 511 keV gamma rays can be constructed. For G = 1/6, e = 0.08 and $N = 5 \times 10^6$, eqn. (2) gives

$$C = 1.1 \times 10^4 \text{ per second.} \tag{7}$$

It is proposed to digitize the coordinates of each event, and store them on magnetic tape. Data transfer to tape at rates of up to $10^5$ words per second is feasible. Successive-approximation analog-to-digital converters with conversion times of less than one microsecond are commercially available (e.g., Sheingold 1972), therefore the coincidence count rate need not be limited by system dead time.

The singles count rate in each chamber will be

$$S = 2GeN = 1.4 \times 10^5 \text{ per second.} \tag{8}$$

For reasons to be described (Chapter 3), a dead time of the order of two microseconds must be associated with the read-out system of each chamber. The proportion of lost counts is given by the probability of an event occurring within this deadtime, T, which follows the detection of an event in either chamber:

$$P = 1 - \exp(-N'T) \tag{9}$$

where $N'$ = count rate in chamber 1

+ count rate in chamber 2

- coincident count rate

$= 2GeN(2-e).$ (10)

When corrected for these deadtime losses, the observed

coincidence count rate will be

$$C' = C \exp(-N'T) \tag{11}$$

i.e. $$C' = 2Ge^2N \exp(-2GeN(2-e)T). \tag{12}$$

This will be a maximum when

$$2(2-e)GeNT = 1 \tag{13}$$

i.e. $$N = 9.8 \times 10^6 \text{ per second.} \tag{14}$$

Thus our estimate of a source strength of 140 microcuries seems a realistic one. With such a source strength, the observed coincidence rate will be

$$C' = 6.4 \times 10^3 \text{ per second,} \tag{15}$$

and the sensitivity, or number of coincidences detected per minute per microcurie, will be

$$s = 1.7 \times 10^3 \text{ counts per min per microcurie.} \tag{16}$$

For the Anger positron camera, a maximum count rate of 1700 per second and a maximum sensitivity of 7000 counts per minute per microcurie (Nuclear Chicago Corporation 1967) are typical. Thus the MWPC positron camera should offer comparable performance to the Anger positron camera.

# CHAPTER 3

# THE MULTIWIRE PROPORTIONAL CHAMBER

## 3.1 History

As the name implies, the MWPC is a gas-filled radiation detector operating in the proportional mode of gas multiplication, and containing a number of anode wires. The chamber is usually rectangular in shape, and the anode wires form a parallel grid. The cathode may be the metal walls of the chamber, or it also may be in the form of one or more planes of parallel wires. When ionizing radiation falls on the chamber an avalanche of electrons is formed by gas multiplication in the region close to an anode wire. By determining at which anode wire the electron avalanche forms, one coordinate of the point at which the chamber intercepted the radiation can be determined. The other coordinate can be determined from the induced pulses on the cathode plane.

In use and construction, the MWPC is similar to the wire spark chambers which have been used for some time for the location of charged particles (Lansiart and Leloup 1963), and from which it was developed. Although the physics of proportional chambers has been well known since the 1930s, and cylindrical proportional chambers using multiwire cathodes (e.g., Watt and Ramsden 1964) or wire mesh anodes (e.g., Rossi and Staub 1949) have long been in

use, it was not until 1968 that the first successful operation of a multiwire proportional chamber as a position sensitive detector was reported (Charpak, Bouclier, Bressani, Favier and Zupancic 1968a). Charpak (1972) has suggested two reasons for this delay. First, early workers did not realize that in order to obtain the gas amplification needed for proportional operation, the anode wires must have a much smaller diameter than the cathode wires. Second, a common belief was that the capacitive coupling between closely spaced anode wires would cause negative pulses to form on more than one wire. The truth is that, due to an effect to be described below, each wire behaves as an independent counter with a sensitive volume of half the distance to its neighbours.

The use of MWPCs in medicine has been largely pioneered by a group at the Lawrence Radiation Laboratory, University of California, Berkeley. Besides the high reliability, simplicity and low cost which make MWPCs suitable for everyday clinical imaging of low energy isotopes, the large area, fast count rates and good spatial resolution make these devices well suited to whole body imaging and fast dynamic studies. MWPCs have been designed for imaging internally administered low energy gamma emitters (Kaufman, Perez-Mendez, Shames and Stoker 1972), for laminographic thyroid imaging by iodine fluorescence (Kaufman, Perez-Mendez, Powell and Stoker 1972), and for neutron radiography (Valentine, Kaplan, Kaufman and Perez-

Mendez 1972). Other suggested biomedical applications are to x-ray fluoroscopy, radioisotope chromatography, and to x-ray crystallography of complex organic molecules (Kaplan, Kaufman, Perez-Mendez and Valentine 1973).

## 3.2 Principles of Operation

The type of MWPC used in this study is shown in Figure 3. In addition to the anode plane, the chamber has two mutually orthogonal "drift planes" and these are used to locate the X and Y coordinates of an ionizing event. These drift planes are at a few hundred volts above ground, while the anode is at a few thousand. The chamber is filled with a heavy gas such as argon or xenon. Wires of diameter 20 microns spaced a few millimetres apart are used for the anode, while wires of diameter 125 microns similarly spaced form the drift planes. The distance between the anode and each drift plane is about 3 millimetres.

For use with low-energy gamma emitters, one or both lead converter foils would be replaced by a thin mylar window, and a collimator would be added. Gamma rays with energies less than about 100 keV will ionize the gas sufficiently to be detected directly. Photoelectrons (and some Compton scattered electrons) will be produced, and will themselves produce secondary electrons by collision with the gas molecules. These electrons drift towards the anode under the influence of the field gradient between anode,

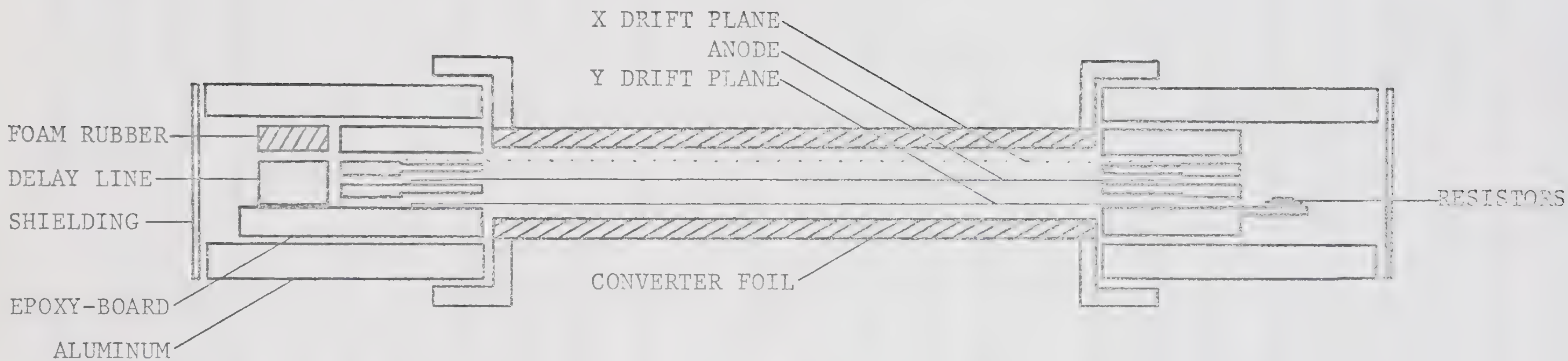


Figure 3: Cross-section of a Multiwire Proportional Chamber

drift plane and cathode (chamber walls). In the region of large field gradient close to each anode wire, the electrons gain sufficient energy to ionize further gas molecules by collision. The avalanche of tertiary electrons formed in this process will be collected by the nearest anode wire, and hence move through a very small change in potential. By contrast, the positive ions drift outwards across the entire potential gradient, inducing a negative pulse on the anode wire and positive pulses on the nearest wires of the outer planes.

Because the positive ions drift outwards in all directions, small positive pulses also appear on the anode wires neighbouring that on which the negative pulse was formed. This effect counteracts the capacitive coupling between the anode wires and makes them behave as independent counters. Thus in general only one anode wire will carry a negative pulse. This effect does not occur on the drift planes and a read-out system which singles out the largest pulse from pulses on a group of wires is required.

When used with annihilation radiation the mechanism is similar, but since the cross-section for ionization of a gas by 511 keV gamma rays is small, lead foils are placed in the entry and exit windows. These foils will produce photoelectric and Compton electrons in both forward and backward directions. These electrons will have energies ranging from zero to hundreds of keV, and will ionize the gas as they pass through it. The secondary electrons

produced by this process will drift to the anode, where an avalanche of tertiary electrons will result in detectable pulses. Since the detection efficiency of a proportional chamber to charged particles of more than minimum ionizing energy is effectively 100%, the overall efficiency to annihilation radiation will be determined by the design and the efficiency of the converter foil.

The gain of the chamber depends on the size and the spacing of the wires, and also on the gas mixture used. A useful discussion of the properties of different chamber gases has been given by Charpak (1970). Electronegative gases produce large multiplications but at the expense of energy resolution. Electrons formed far from the anode are likely to be captured, and hence the gain is not constant throughout the chamber (Bouclier, Charpak, Dimcovski, Fischer, Sauli, Coignet and Flugge 1970). However, it is sometimes advantageous to add gas such as ethyl bromide to argon to decrease the sensitive zone around a wire (Grunberg, Cohen and Mathieu 1970). It is preferable not to use pure argon in the chamber because the addition of a small percentage of oxygen will cause appreciable electron losses. However, these losses will be substantially diminished if a few percent of carbon dioxide or isobutane is present (Charpak 1970). With argon - carbon dioxide or argon - isobutane mixtures, gas amplification of the order of $10^6$ is normally achieved. However, a "magic" gas mixture (argon, isobutane and freon) which gives amplifications of

$10^8$ has been reported (Bouclier, Charpak, Dimcovski, Fischer, Sauli, Coignet and Flugge 1970). A second "magic" gas mixture (argon, xenon and carbon dioxide) has since been reported by Fuzesy, Jaros, Kaufman, Merriner, Parker, Perez-Mendez and Redner (1972).

A useful discussion of the optimum spacing, diameter and material of the chamber wires has been given by Wynchank (1970). He recommends gold-plated tungsten wire because of its high tensile strength and ease of soldering. Stainless steel wire is preferable because of its better uniformity, but is difficult to solder. However, it has been successfully used by Parker, Jones, Kadyk, Stevenson, Katsura, Peterson and Yount (1971).

The wires are in unstable equilibrium and the minimum tension required to prevent alternate displacement above and below their equilibrium position has been calculated by Trippe (1969):

$$T = C^2V^2L^2/S^2, \qquad (1)$$

where C, V, L and S are the capacity per unit length, the voltage, the distance between wire planes and the spacing of the wires respectively. For 20 micron wires 25 cm long, spaced 2 mm apart and with 2000V them and the drift plane wires 3 mm away, this minimum tension is approximately 8 gm wt. This is far below the yield point of tungsten wire (55-60 gm wt for a 20 micron wire).

## 3.3 Read-out Schemes

When radiation is detected by the chamber, a large positive pulse is induced on the wire of each drift plane closest to the ionizing event, and smaller pulses are induced on the next closest wires. In order to obtain the spatial coordinates of the event, one must determine which wire carries this large pulse. The simplest method is to provide an amplifier and discriminator for each wire. The outputs of these discriminators are passed through decision logic and stored. Although expensive, this approach has been used for large systems requiring fast read-out to a computer (Cunitz, Sippach and Dieperink 1970). A powerful but economic system of decision logic has been described by Pages (1970).

Several schemes to cut down the number of amplifiers and discriminators have been proposed. Some of these have been summarized by Charpak, Bouclier, Bressani, Favier and Zupancic (1968b). One scheme uses ferrite core transformers to divide the wires into subgroups; subsequent transformers locate the pulse-carrying wire within the subgroup. A scheme that has been borrowed from spark chambers is to connect inductors between the wires, so that with the stray capacitances of the wires a lumped constant delay line is formed. By comparing the time of arrival of the pulses at either end of this delay line, the pulse-carrying wire can be located. A development of this method is based on the

fact that the pulses are attenuated as they pass along the delay line. Thus one can simply separate the wires by small resistors and compare the amplitudes of the pulses at either end.

A simple and elegant read-out scheme, which we have adopted for our wire chambers, involves the use of distributed constant electromagnetic delay lines capacitively coupled tc the wires (Rindi, Perez-Mendez and Wallace 1970). The delay lines developed by Grove, Ko, Leskovar and Perez-Mendez (1972) have a flat profile, so that they may be clamped to the copper lands of a printed circuit board to which the drift plane wires have been soldered. The time lag between the arrival of a pulse on a drift plane wire and its arrival at the end of the delay line depends on the pcint at which the pulse was coupled into the delay line, that is, on the position of the wire (Figure 4). Moreover, since the delay lines are of the distributed constant type, pulses from neighbouring wires combine in the delay line to give a composite pulse whose centroid represents the pcsition of the ionizing event. Thus by triggering cn the centroid of the pulse, the interpolation cf events which occur between wires is automatically effected.

Spatial positions have now been translated into time-delays, but in order to drive a display they must be translated into voltages. The Time-to-Amplitude Converters (TACs) used for this are basically capacitors which are

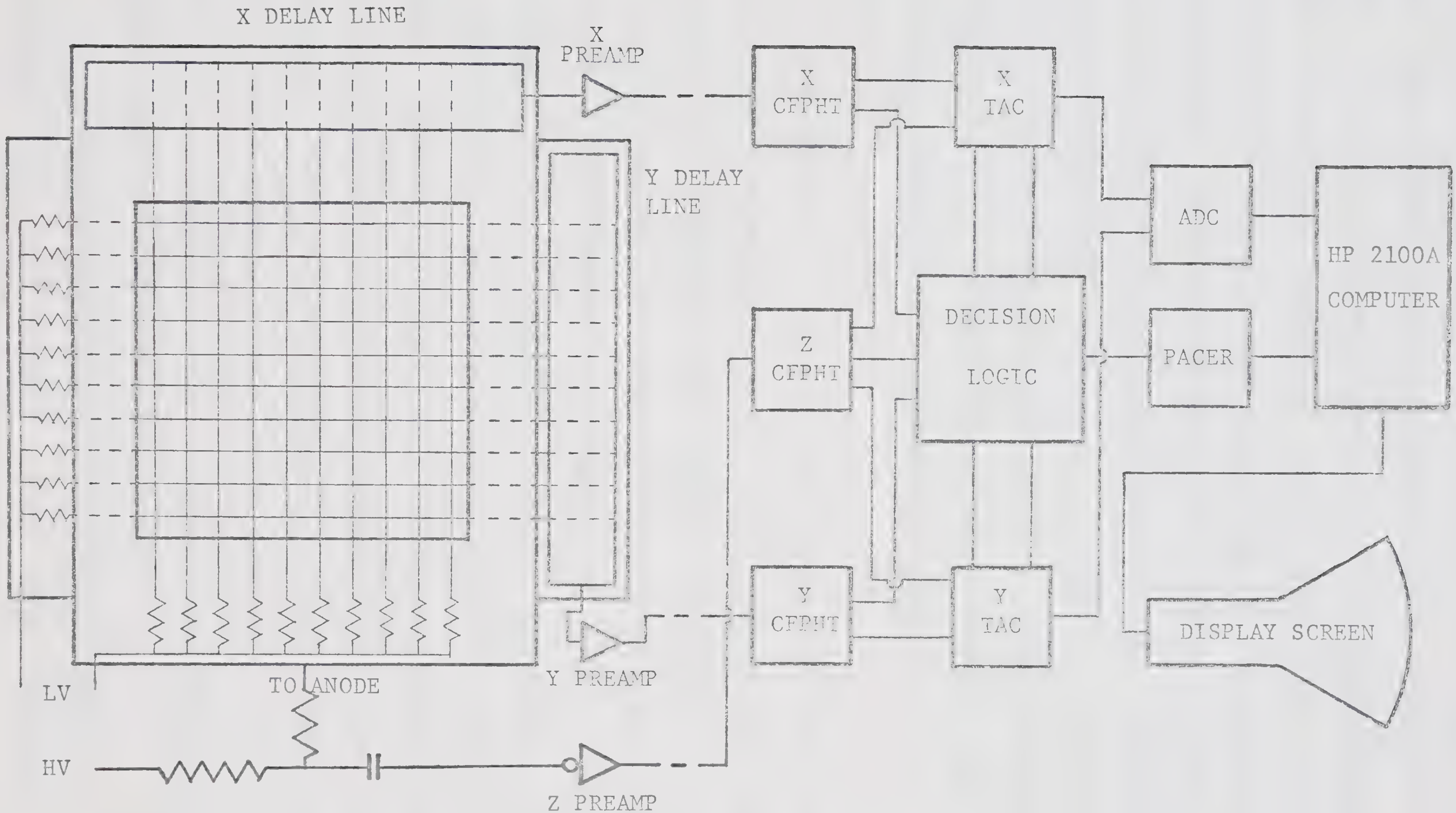


Figure 4: Read-out Scheme for MWPCs using a Digital Computer

charged from a constant current source. A pulse from the anode wires (which are all connected to a common bus bar) is used to turn on the current, and the corresponding pulse from a delay line turns it off. Since the current is constant, the voltage appearing across the capacitor will be proportional to the time for which it was switched on, and hence to the position of the ionizing event. These voltages can be digitized and read into a computer. Alternatively, they can be applied to the plates of an oscilloscope (with a suitably timed Z-unblank pulse) to make a dot appear on the screen at a position corresponding to that of the ionizing event.

In practice, a few more elements are needed in a simple read-out scheme, such as that shown in Figure 4. Starting and stopping the TACs at the right time requires accurately locating the peaks of the anode pulses and the centroids of the delay line pulses. To preserve the spatial resolution of the chamber requires accuracies of a few nanoseconds, so Constant Fraction of Pulse Height Trigger (CFPHT) circuits are used to produce fast trigger pulses at the correct point of the input pulse. With gamma emitting isotopes, Pulse Height Analysis circuits built into the CFPHTs can be used to reject any pulses which do not fall within the dynamic range expected from the energy of the isotope, thus reducing the background.

The use of delay lines for read-out imposes a longer dead-time on the system than other methods: a few

microseconds are required for a pulse to traverse the delay line and be detected. If a second "start" pulse arrives from the anode before the "stop" pulse corresponding to the first "start" pulse has traversed the delay line and been detected, a "pile-up" condition exists. It is then impossible to determine to which "start" pulses the "stop" pulses correspond, and the pulses will not produce valid data. A Decision Logic Unit rejects the data in the event of such pile-up. This unit acts as a controller for the whole system and can be used to reject other invalid or incomplete data, drive a scalar, and send the appropriate commands to the computer.

# CHAPTER 4

# DESIGN AND CONSTRUCTION OF THE CAMERA

## 4.1 The System

An MWPC positron camera requires the following hardware elements: wire chambers sensitive to annihilation radiation, a read-out system, a decision logic unit to control the read-out system and reject invalid data, a coincidence unit, and a means of digitizing the raw data and transferring them to the computer. In addition, software is required to acquire and analyse the data and produce a display.

In our imaging system, each wire chamber uses a read-out scheme like that shown in Figure 4. The Decision Logic Units and the Coincidence Unit are combined to form a System Controller. Digitizing is performed by a commercial analogue-to-digital converter (Hewlett Packard 5610A), which is controlled through a Pacer (Hewlett Packard 5611A). The computer (Hewlett Packard 2100A) is used on-line to acquire the data, which are stored in a chained-buffer system to facilitate transfer to magnetic tape. At a later time the tape is replayed, the data are analysed and the display is generated. Because no reduction of the data is performed prior to this time, any "plane of best focus" or region of interest can be displayed.

The sequence of events is as follows: if it decides

that the data accumulated in the TACs are valid, the Controller makes an appropriate command to the Pacer, which results in the digitizing of the data. After a short time has elapsed to allow the data to be digitized and stored in a buffer, CLEAR and RESET pulses are sent from the Controller to the TACs to destroy the data and permit the detection of a new event. If the data are not valid, either because incomplete, or no coincidence occurred, or a pile-up condition exists, the command to the Pacer is not sent and the TACs are cleared and reset as soon as the system is ready to receive another event.

A detailed description of the design and construction of each component of the system will now be given.

## 4.2 Design and Construction of the MWPCs

The design of an MWPC sensitive to annihilation radiation has some features in common with the neutron-sensitive chambers that have been reported by Valentine, Kaplan, Kaufman and Perez-Mendez (1972). In both cases the sensitivity is increased by the addition of a converter foil. In the case of annihilation radiation, a high Z material is used to produce photoelectric and Compton scattered electrons when 511 keV gamma rays fall on it. Although there is some evidence that such electrons are forward-peaked (Chatterjee, Draper, Howells and Osman 1973), many electrons will traverse the chamber obliquely to the

path of the incident gamma ray, degrading the spatial resolution. To minimise this loss of resolution it is necessary to keep the chamber as thin as possible. Other general design considerations are that all parts should be easily and inexpensively machined, and the whole should be easily assembled and dismantled. Although a continuous flow gas system is used, the chambers should be nearly gas tight. Finally, the converter foils should be readily demountable so that improvements to their design can be made and tested.

Although one of the advantages of an MWPC positron camera is the possibility of using large area detectors, it was decided to construct the prototype on a small scale. The active area of each chamber is 25 cm square. Also, we decided to forgo the construction of shaped converter foils until the feasibility of the system had been proven. Flat sheets of lead are used for the conversion. The design adopted is illustrated in Figure 3. The wires are supported on frames of Nema G-10 fibre-glass epoxy-board, which are stacked and clamped between aluminum backing-plates carrying the converter foils. O-rings are used between the boards to prevent major gas leaks. The drift planes are approximately 3.2 mm from the converter foils, and the anode plane is 3.2 mm from the drift planes; thus the active thickness of the chamber is approximately 12.8 mm. Electrostatic shielding surrounds the edges of the chamber, and is used for mounting gas valves and electrical connectors.

In order to achieve high field gradients, wires of

diameter 20 microns spaced 2 mm apart are used for the anode. The outer planes are 125 micron diameter wires spaced at 1 mm. For the anode, we used gold-plated tungsten wire under a tension of 40 gm wt, which is approximately 60% of its tensile strength. For the thicker cathode wires, we used a copper-beryllium alloy wire tensioned at 150 gm wt. To reduce the fringe field effects occurring at the edges of the anode plane, extra wires are included at each side of the active area. Thus any slight bowing of these wires due to the unbalanced electrostatic forces will not affect the performance of the chamber. The epoxy-board frames that support the wires also carry printed-circuit boards to which the wires are soldered. These circuits supply power to the wires and transfer the pulses to the preamplifiers. The anode-plane circuit-board carries the components of an RC network which shapes and decouples the pulses. The outer plane circuit-boards connect each wire at one end through a 200K-ohm isolating resistor to a common voltage supply, and at the other to a wide copper land which passes under the delay line. For efficient coupling to the delay-lines, the copper-lands are made double-width and two outer plane wires are connected to each land.

### 4.2.1 Construction of Wire Planes

The wires in each plane must be correctly tensioned, be accurately coplanar, and be precisely spaced. This was

accomplished by means of the machine shown in Figure 5, which was designed and built at the University of Alberta Nuclear Research Centre and kindly made available to us. The wire is drawn from its spool as a continuous thread. Tensioning is achieved by a feedback mechanism (Figure 6): a beam of light passes through a grey wedge attached to a weight supported by the wire, and falls on a photocell. The output of this photocell drives a servo-motor which turns the spool of wire.

The wire is threaded through a pulley system mounted on a shuttle, and the free end is attached to the frame of the apparatus. The epoxy-board frame, with circuit-board attached, is laid flat on a metal table in the centre of the apparatus, so that the continuous wire can be "woven" into a parallel grid above it. Along each side of the apparatus are located holes into which steel pins can be inserted. The diameter and spacing of these pins is equal to the desired wire spacing. The wire is drawn across the apparatus with the shuttle, a pin is inserted in front of the wire, the wire is returned in front of the pin and brought to the other side of the apparatus, and the operation is repeated until enough wires to span the active area have been stretched above the frame. Then accurately machined vee-shaped threads are raised from beneath the wires on either side of the apparatus so that the wires fall into the vees. This insures that the wires are correctly spaced and accurately coplanar. The epoxy-board frame can

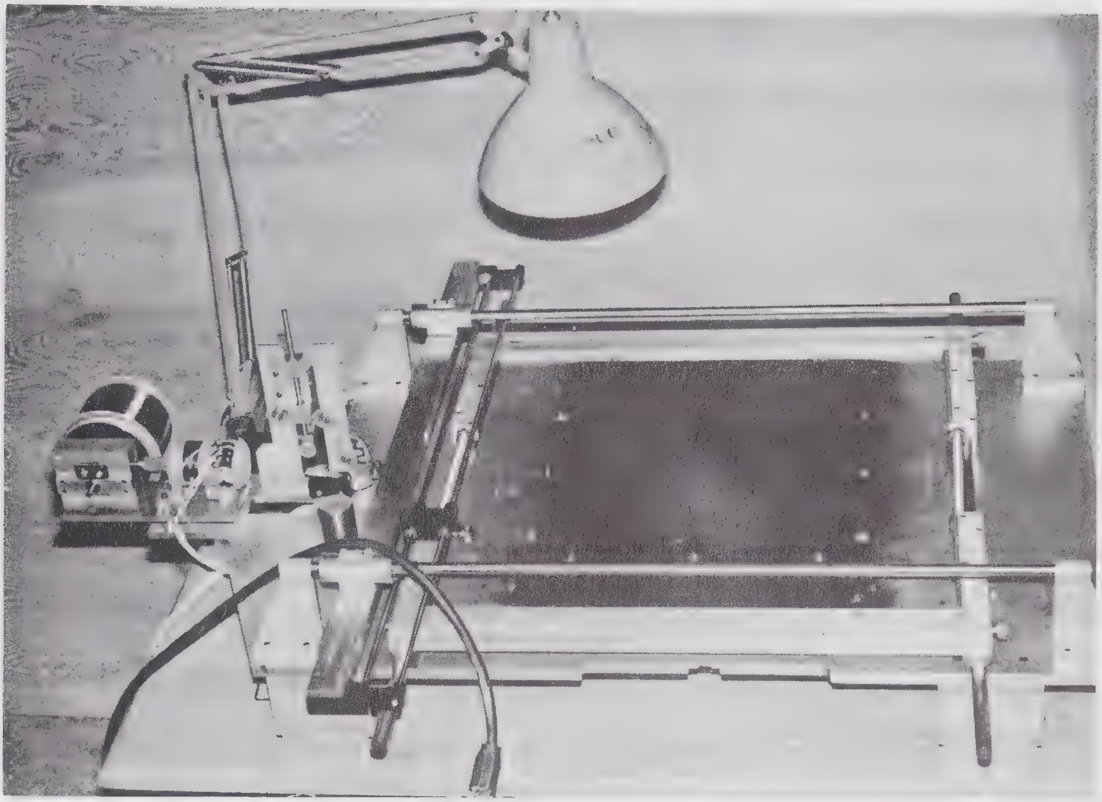

Figure 5: Machine for Constructing Wire Planes

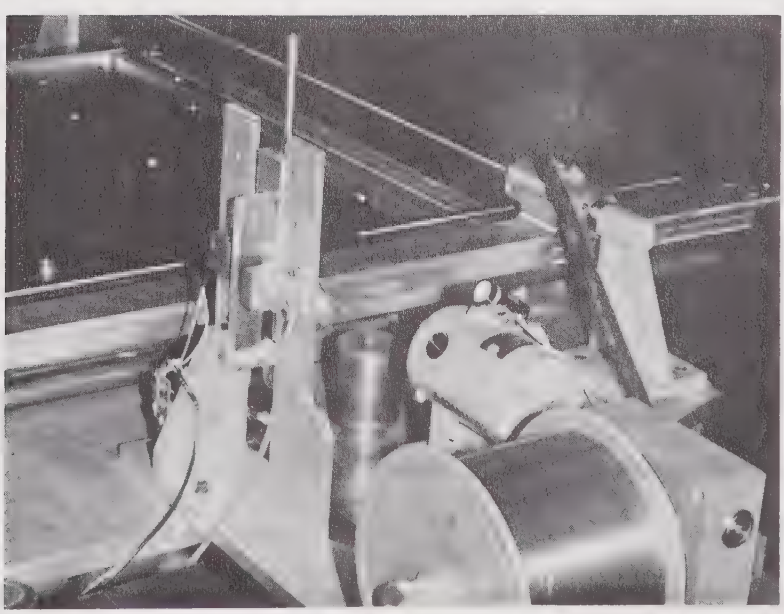

Figure 6: Detail of Servocontrol Mechanism

now be positioned precisely beneath the wires and raised until the copper lands just contact them. The wires are then securely fastened to the frame with a low viscosity epoxy (Eccobond 24, Emerson and Cuming Inc.), which is run into a groove under the wires. This prevents any inadvertant movement of the wires when soldering. When the epoxy has cured, the wires can be soldered to the copper lands. For the gold-plated wires this requires a cool iron, as the gold-plating will flake off if overheated. A mixture of Kester soldering paste and peanut oil makes a suitable flux. When the soldering is complete, the excess wire can be cut off with a sharp scalpel, and the flux removed with xylene followed by acetone. Components such as resistors and capacitors are added to the boards and the wire planes are ready for service.

### 4.2.2 Converter Foils

The function of the converter foils is to produce electrons when struck by annihilation radiation. A material with high Z is required and lead is usually chosen because it is inexpensive and easy to machine. Although aware that the development of shaped converter foils was in progress (Kaufman, private communication), we chose plane lead foils for our prototype system. The optimum thickness of the foil is a compromise: a thick foil will convert more gamma rays but fewer of the electrons will emerge to ionise the gas.

The situation is complicated by the fact that both photoelectric and Compton scattered electrons will be produced with a wide range of energies. Although the range of 511 keV electrons in lead is 80 microns, the thickness for which most electrons escape has been estimated as 67 microns by Chatterjee, Draper, Howells and Osman (1973); however, for convenience, somewhat thicker foils were used. To construct the foils, a sheet of lead 3.2 mm thick was epoxied to a 1.6 mm thick sheet of aluminum to provide rigidity, then the surface was milled flat, so that the final thickness of lead was about 2.5 mm. (For comparison, the mean free path of 511 keV gamma rays in lead is 5.94 mm). The foils were mounted on rigid frames and the entire units recessed into the chamber to bring the inner surface of the foils to within 3.2 mm of the drift planes. Foils were used in both entry and exit windows of the chambers, since back-scattered electrons are expected.

### 4.2.3 Delay Lines

Delay lines specially designed for wire chamber read-out are now commercially available (Radiation Technology Assoc., 17 Calico Tree Road, Hauppauge, N.Y.). These delay lines have a rectangular cross-section (see Figure 7) which enables them to be capacitively coupled to the wires simply by clamping them to circuit-board lands to which the wires have been soldered. We used a mylar dielectric between the

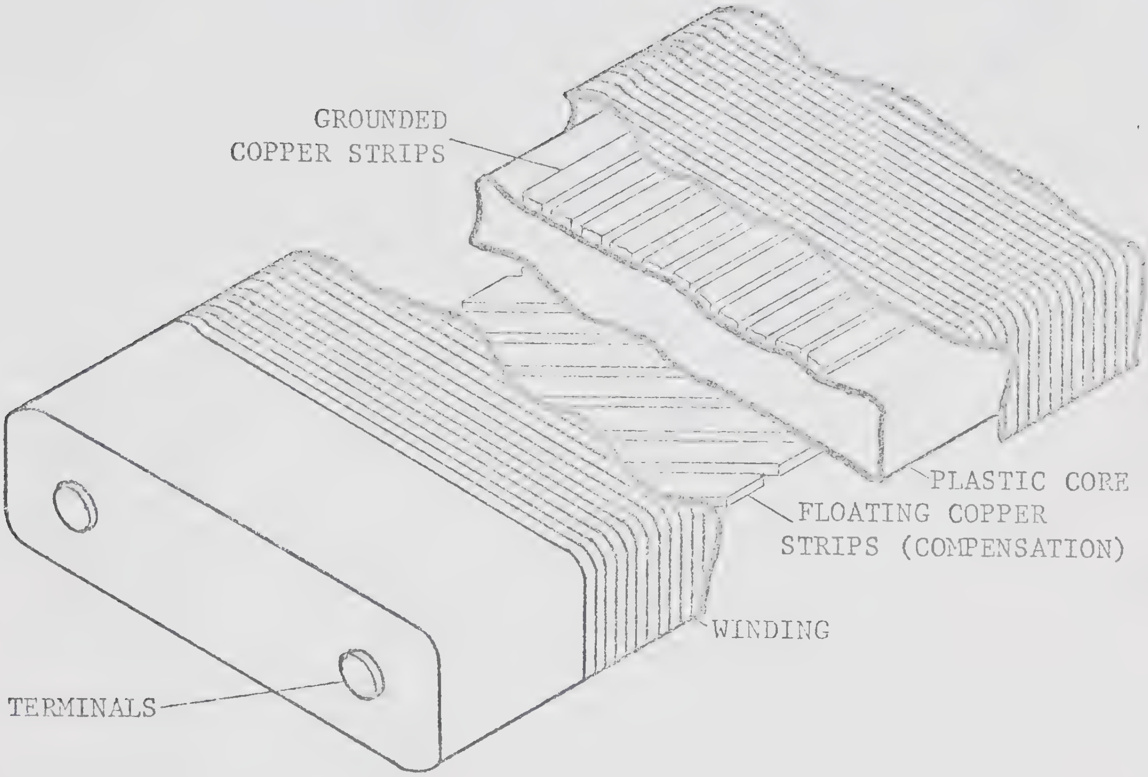


Figure 7: Cut-away Drawing of Delay Line

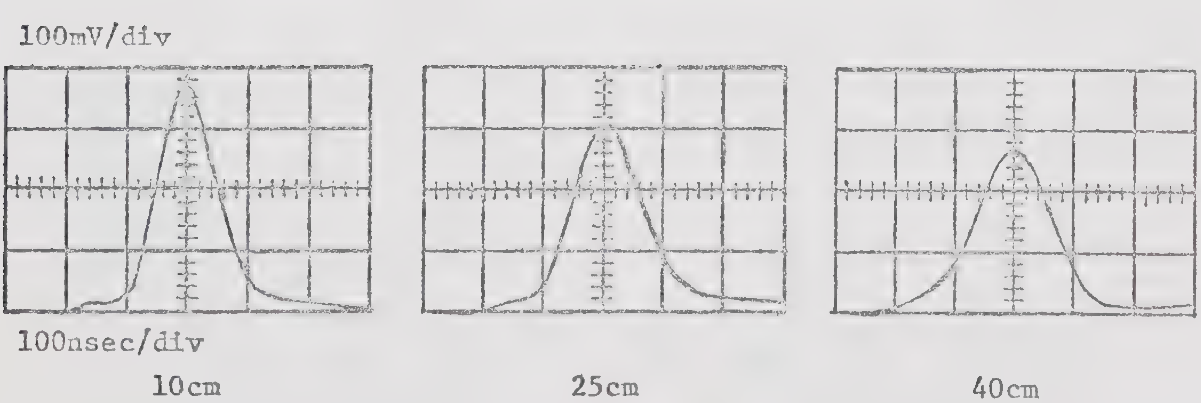


Figure 8: Change of Shape of Pulses Coupled
into Line at Different Distances
(After Grove, Ko, Leskovar and Perez-Mendez 1971)

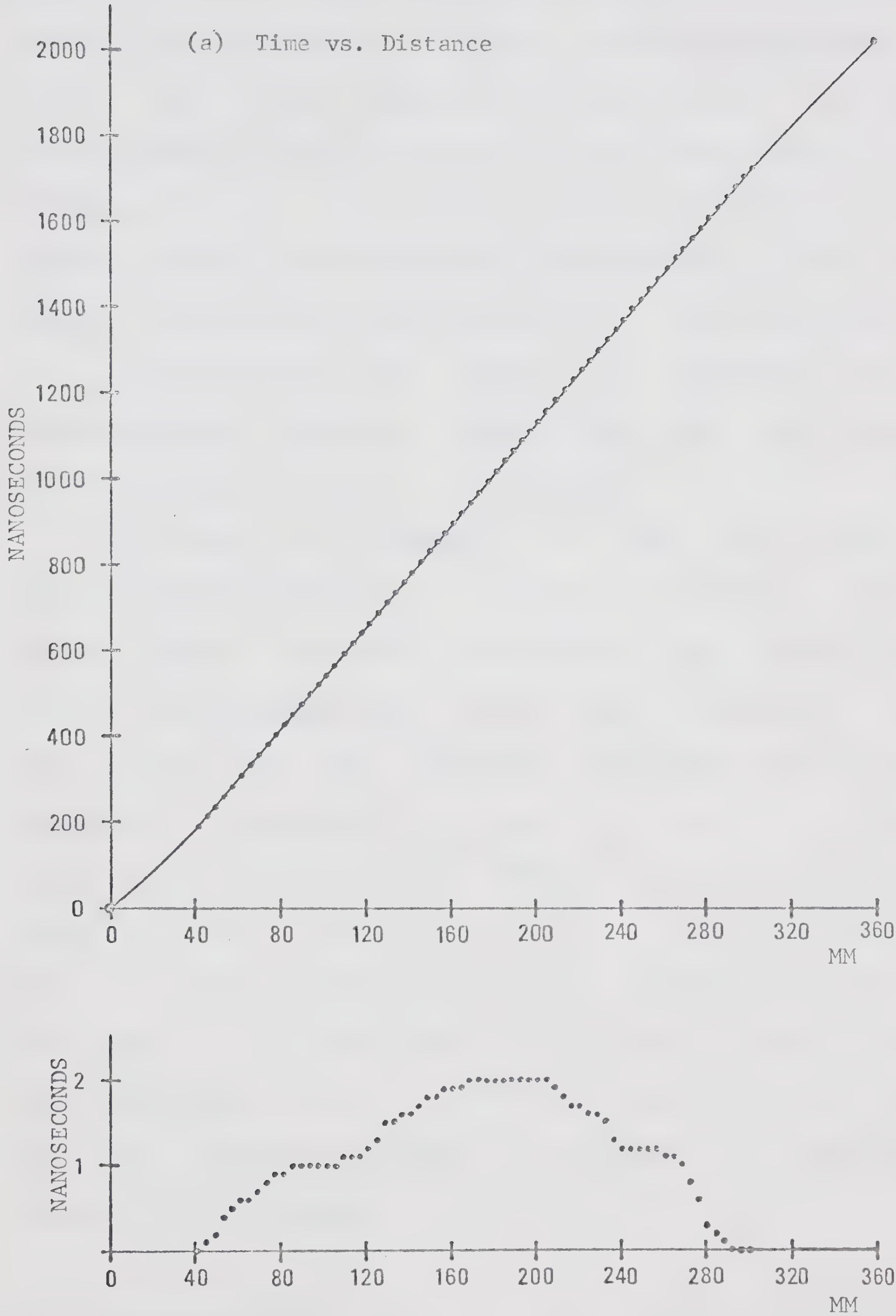


(b) Departure from Linearity in Central Region

Figure 9: Linearity of Delay Lines

delay lines and lands, and a strip of foam rubber to hold them in place and apply a uniform pressure throughout their length. The lines used are 35 cm in length. To allow for any nonlinearity due to change in parameters toward the ends of the line, only the central 25 cm is coupled to the chamber wires. The departure from linearity in this central region is two nanoseconds (Figure 9). The total delay time is 2 microseconds. The lines are terminated in their characteristic impedance (about 1200 ohms) and grounded at the end furthest from the preamplifier.

The design and properties of these delay lines have been extensively described by Grove, Kc, Leskovar and Perez-Mendez (1972) and Grove, Perez-Mendez and Sperinde (1973), and will be reviewed only briefly here. Dispersion due to the decrease of the effective inductance with increasing frequency is compensated through the use of a "floating patch", and a bandwidth of 3 MHz is achieved. The delay to risetime ratio is approximately 30. Figure 8 shows the shape of the output pulses for different input pulse positions. It will be seen that the area of the pulse is less attenuated than the pulse amplitude. For this reason, the most accurate timing information is obtained by integrating the pulses.

#### 4.2.4 Preamplifiers

The preamplifiers bring the pulse amplitudes to a

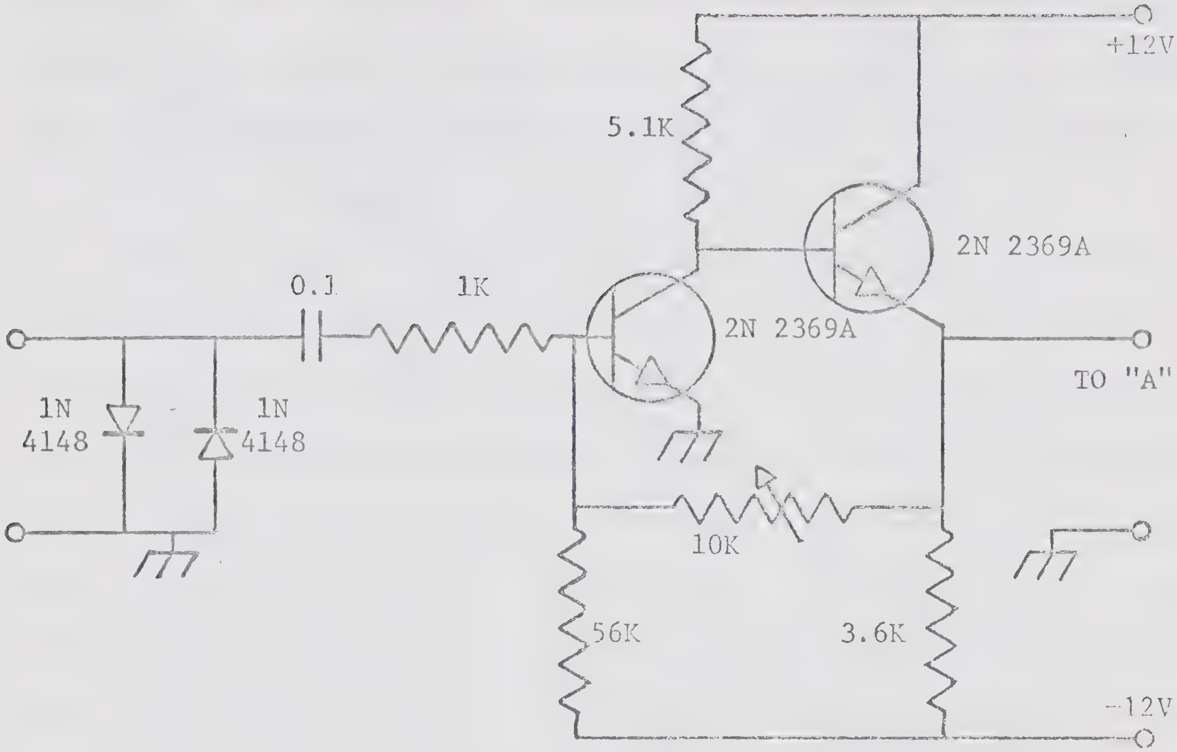


(a): Extra Stage for Anode Preamps

(b): Drift Plane Preamps

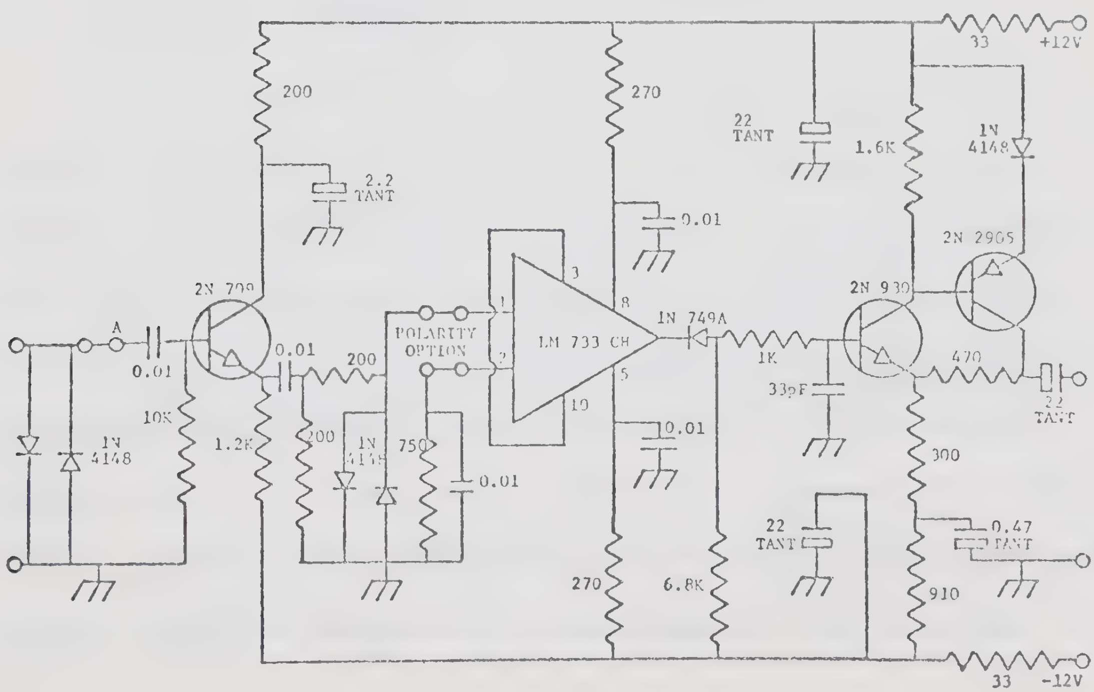


Figure 10: Circuit Diagram of Preamplifiers

level suitable for processing by the read-out system. In addition, they provide an output impedance low enough to drive 50 ohm cable, discriminate against pulses of the wrong sign and protect the read-out system from large, spurious pulses due to sparking.

The circuit adopted is shown in Figure 10. The final stages of the amplifiers - and also the CFPHTs and TACs - are based on circuits kindly made available by the Lawrence Radiation Laboratory, Berkeley. Large pulses are clipped by the crossed diodes. Pulses from the anode plane are smaller than those from the drift planes, and an extra stage was added to the anode preamplifier to compensate for this. The gain of the drift-plane amplifiers is approximately 30, and that of the anode plane amplifiers 100. The noise from all preamplifiers is less than 20 millivolts.

### 4.2.5 Chamber Assembly

In assembling the wire chambers, cleanliness is the primary objective. A room without air-conditioning was chosen to minimise the motion of dust particles in the air. The boards were carefully cleaned with methyl alcohol and the wires inspected for dirt or corrosion. The O-rings were installed with a small amount of silicon vacuum grease. The delay lines and associated wiring were inserted and the four bolts holding the backing plates together tightened with a torque wrench to ensure even pressure on the O-rings. The

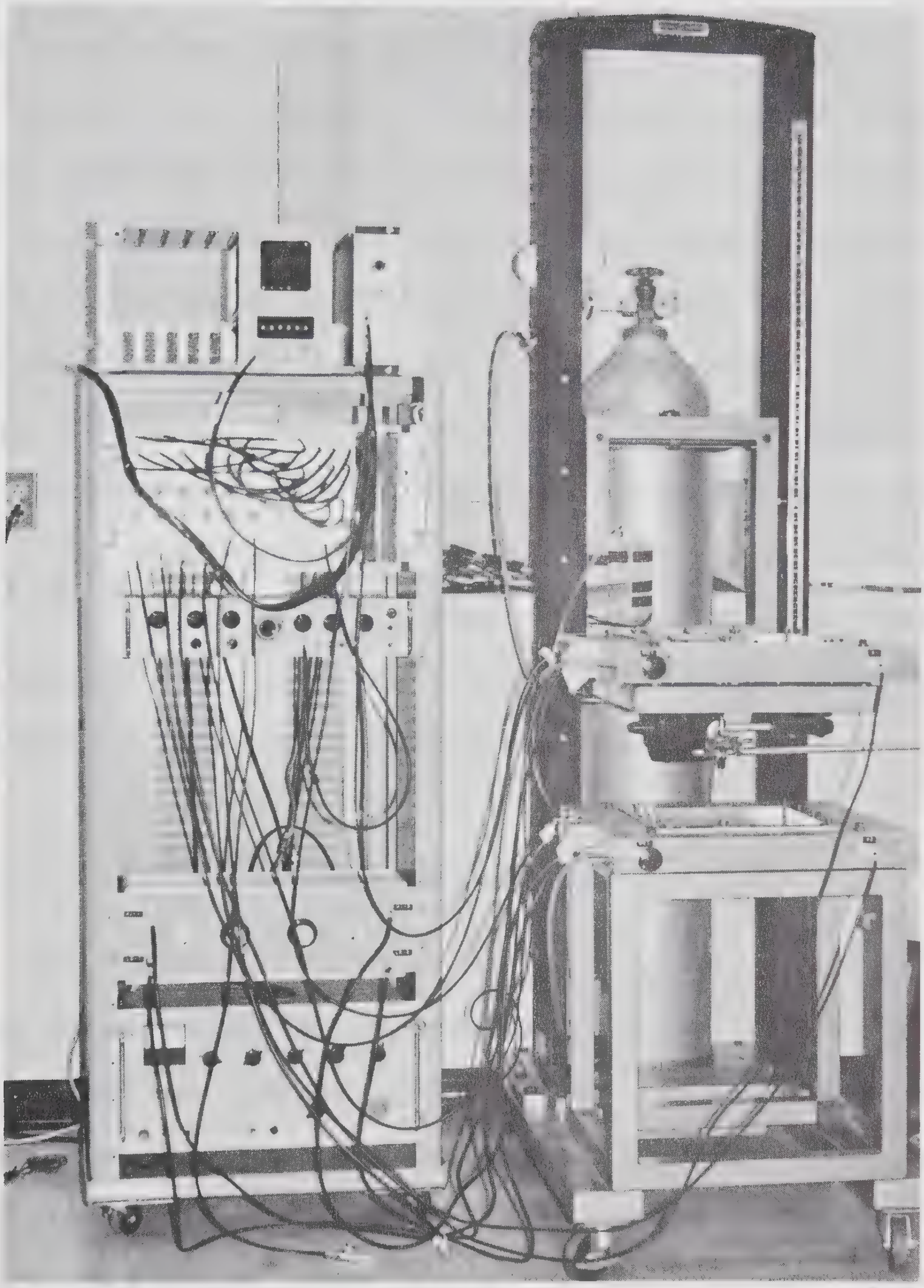

Figure 11: General View of Wire Chambers

gas valves, preamplifiers and electrostatic shielding were inserted and the complete wire chambers mounted on a stand, allowing the distance between them to be continuously varied while keeping the faces parallel (see Figure 11).

Since the volume of the chamber is about 500 cc, an initial gas flow rate of 100 cc per minute for about half an hour is adequate to flush out the air. Dust particles which remain on the wires can often be removed by applying a negative voltage to the anode. The gas is 93% argon with 7% carbon dioxide, and a flow rate of 1 cc per minute can be used for normal operation. With an anode potential of 2000 volts and drift plane potential of 100 volts, this results in pulses (after amplification) of up to two volts in amplitude. The chambers enter the Geiger mode if anode potentials of more than 2050 V are used.

### 4.2.6 The High Voltage Power Supply

The variable voltage divider shown in Figure 12, driven by a commercial high-voltage supply (Fluke 408B), was constructed to supply 2000 volts to the anode of each chamber and one twentieth of this to the drift planes. Since the gain of a proportional counter is particularly voltage sensitive, the anode voltage must be well stabilised, but it is convenient to vary the anode voltage of one chamber independently of the other to compensate for minor differences in gain due to other factors. Because of

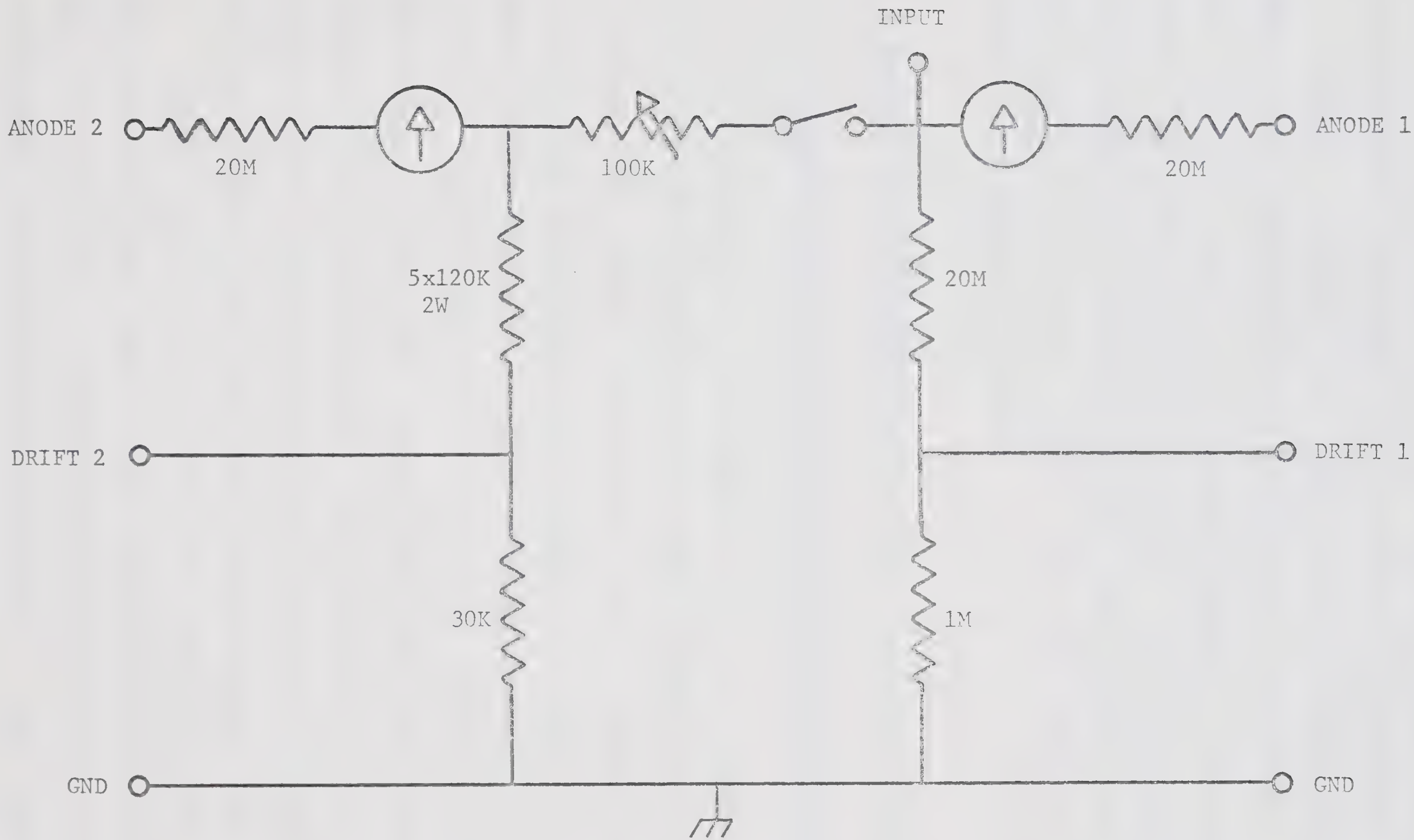


Figure 12: Divider Network for High Voltage Supply

the high voltages involved, all controls have insulating shafts and all components are mounted on a plexiglass board. To minimise "pulling" of the divider voltage by chamber current, the current flowing through the divider is about one thousand times the chamber current. Microammeters indicate an excessive chamber current due to sparking or total ionisation (discharge) of the gas; in this event or in the event of a short circuit due to a broken wire, the current is resistance limited.

## 4.3 Design and Construction of the Read-out System

### 4.3.1 Constant Fraction of Pulse Height Trigger Circuits

The CFPHT is a development of the clipping stub crossover timing technique (Orman 1963), which has been used to avoid the "walk" associated with a fixed threshold discriminator (Figure 13a,b). Triggering occurs when the pulse has risen (or fallen) to a certain fraction of its maximum, rather than at the maximum itself. This is advantageous when the maximum of the pulse does not represent the point of optimum time resolution. The CFPHT provides more reliable triggering for small fractions than does the clipping stub technique (Gedcke and McDonald 1967).

Pulses received from different parts of the delay lines used for MWPC read-out are more nearly uniform in area than in amplitude. By integrating these pulses we obtain pulses which are fairly uniform in shape. The maximum of

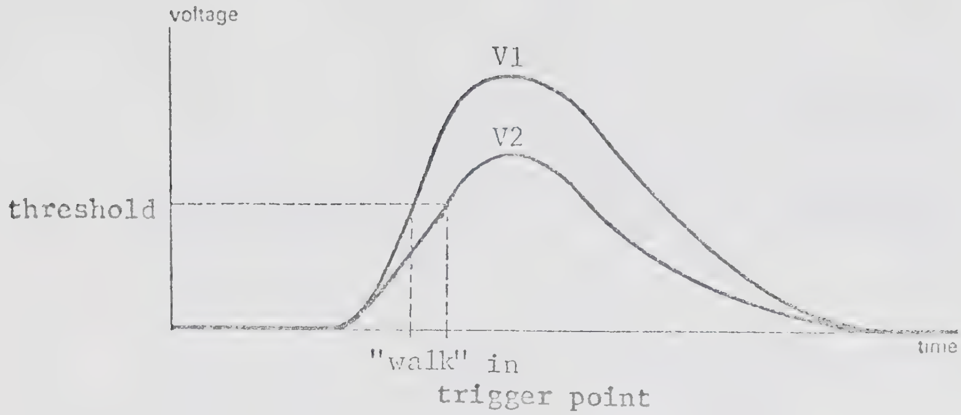


(a): Fixed Threshold

(b): Constant Fraction

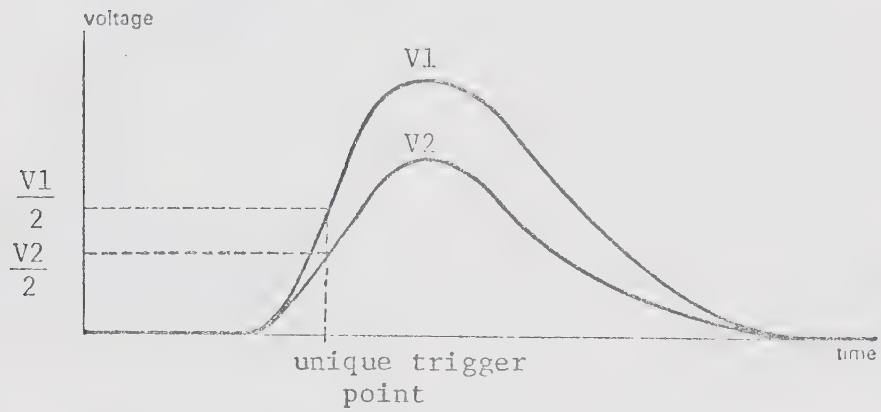


Figure 13: Fixed Threshold and Constant Fraction Triggering

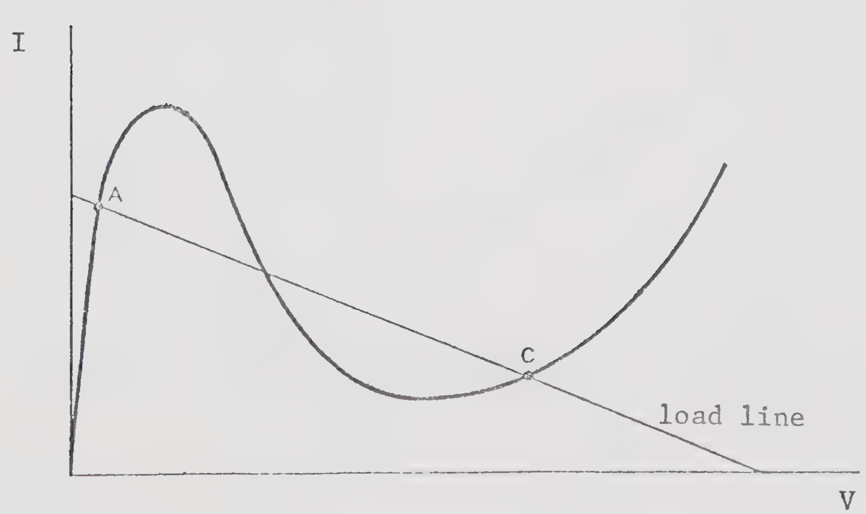


Figure 14: Tunnel Diode Characteristic
(After Delaney 1969)

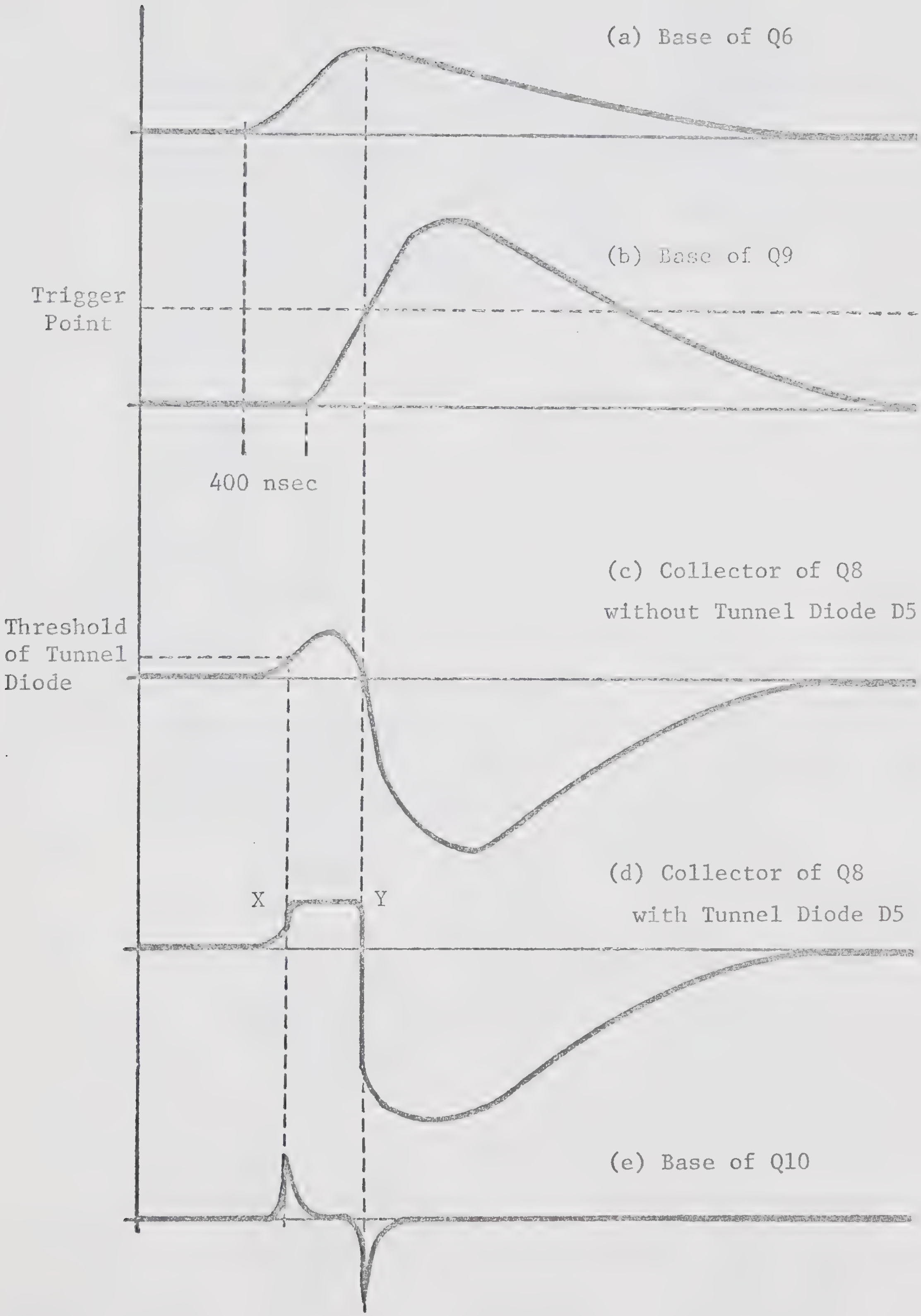


Figure 15: Time Sequence Diagram of Operation of CFPHTs

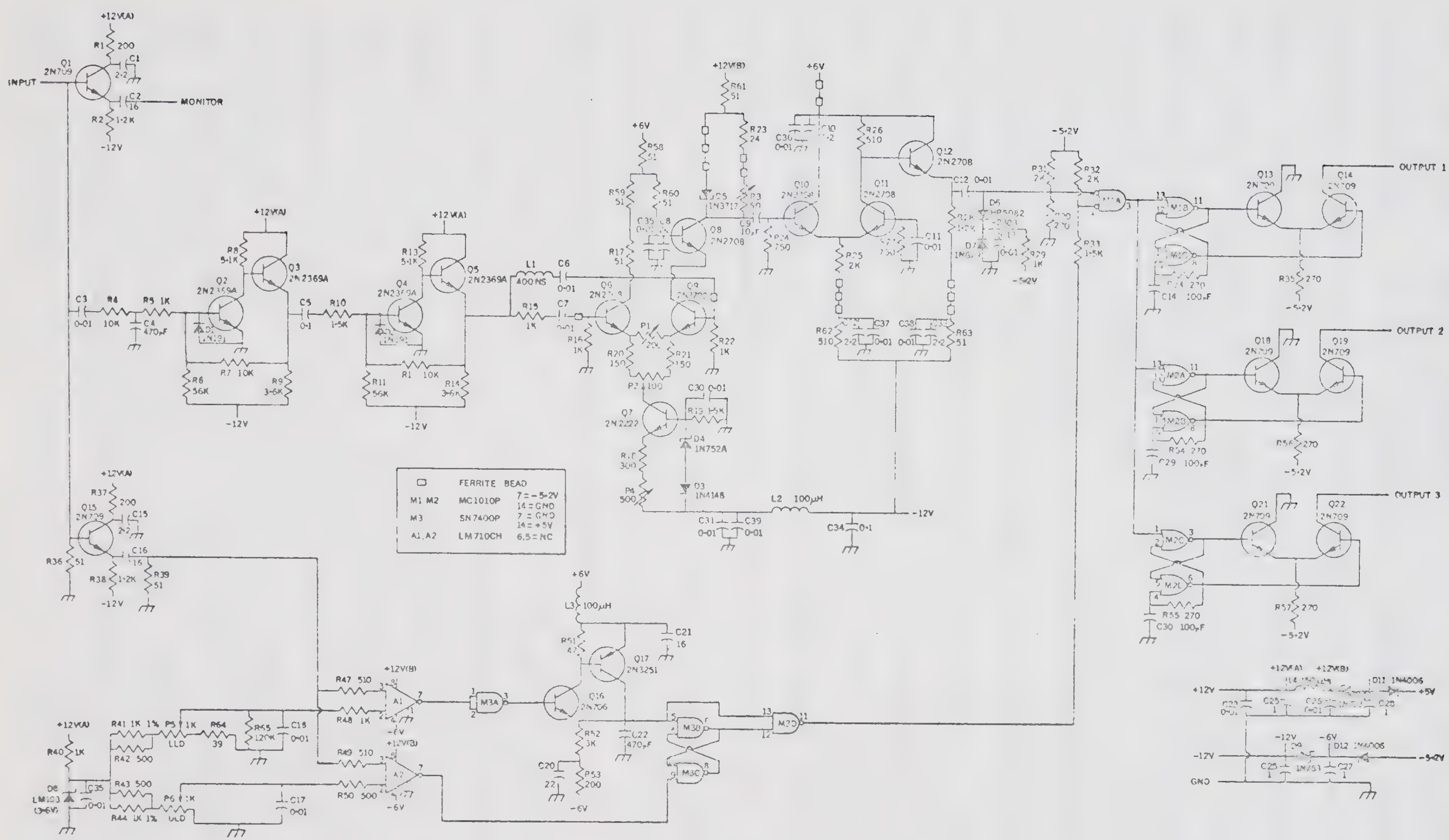


Figure 16: Circuit Diagram of CFPHTs

the original pulse corresponds to the 50% point on the leading edge of the integrated pulse. Because the integrated pulses are the same shape, the time to rise from zero to a given fraction of the maximum will be the same for all pulses regardless of their amplitudes. Thus for delay line read-out, a CFPHT triggering at 50% of the maximum will give optimum time resclution.

A circuit diagram of the CFPHT, as modified for use in our system, is shown in Figure 16. The input signal is integrated by the network formed by R4 and C4. The signal follows two paths: in one path its amplitude is halved by the voltage divider formed by R15 and R16, in the other it passes through a 400 nanosecond delay line. The value of this delay is the time required for the signal to rise to 50% of its maximum (Figure 15b). The two signals are fed to a difference amplifier (Q6, Q9) and the point at which the output crosses zero is the triggering point.

A tunnel dicde (D5) is used to locate this crossover point accurately, as it has the effect of increasing the slope of the waveform. The tunnel diode is biased so that its operating point is normally at point "C" of its characteristic (see Figure 14). Since its anode is tied to the positive rail, increasing the voltage on its cathode will cause the vcltage across the diode to decrease, until the operating point transfers to "A". This "arming" happens very rapidly and as a result the waveform rises sharply at point X of Figure 15d. When point Y is reached, the voltage

across the diode starts to rise again and the operating point resets to "C", causing the waveform to cross zero very sharply. The signal is then differentiated, giving the pulses shown in Figure 15e: the positive pulse is suppressed by a diode (D6), and the negative pulse becomes the trigger pulse.

The lower half of the circuit comprises two variable threshold discriminators, which ensure that only pulses lying within a specified range of amplitudes are accepted. When the wire chamber is used for imaging gamma-emitting isotopes, this Pulse Height Analysis can be used to reduce the effects of background radiation. When a converter foil is used this is no longer possible and the discriminators are not used. In the absence of an inhibiting pulse from these discriminators, the trigger pulse is amplified, lengthened by monostable multivibrators, and fed to low impedance outputs.

### 4.3.2 Time to Amplitude Converters

The function of these devices is to produce a voltage which is proportional to the elapsed time between the "start" and "stop" pulses from anode and delay line respectively. Two TACs are incorporated into each unit: one for the X coordinate and one for the Y; the same Z pulse starts both. The circuit for the TACs is shown in Figure 17. Since the operation of the X TAC and Y TAC is

Figure 17:

Circuit Diagram of TACs

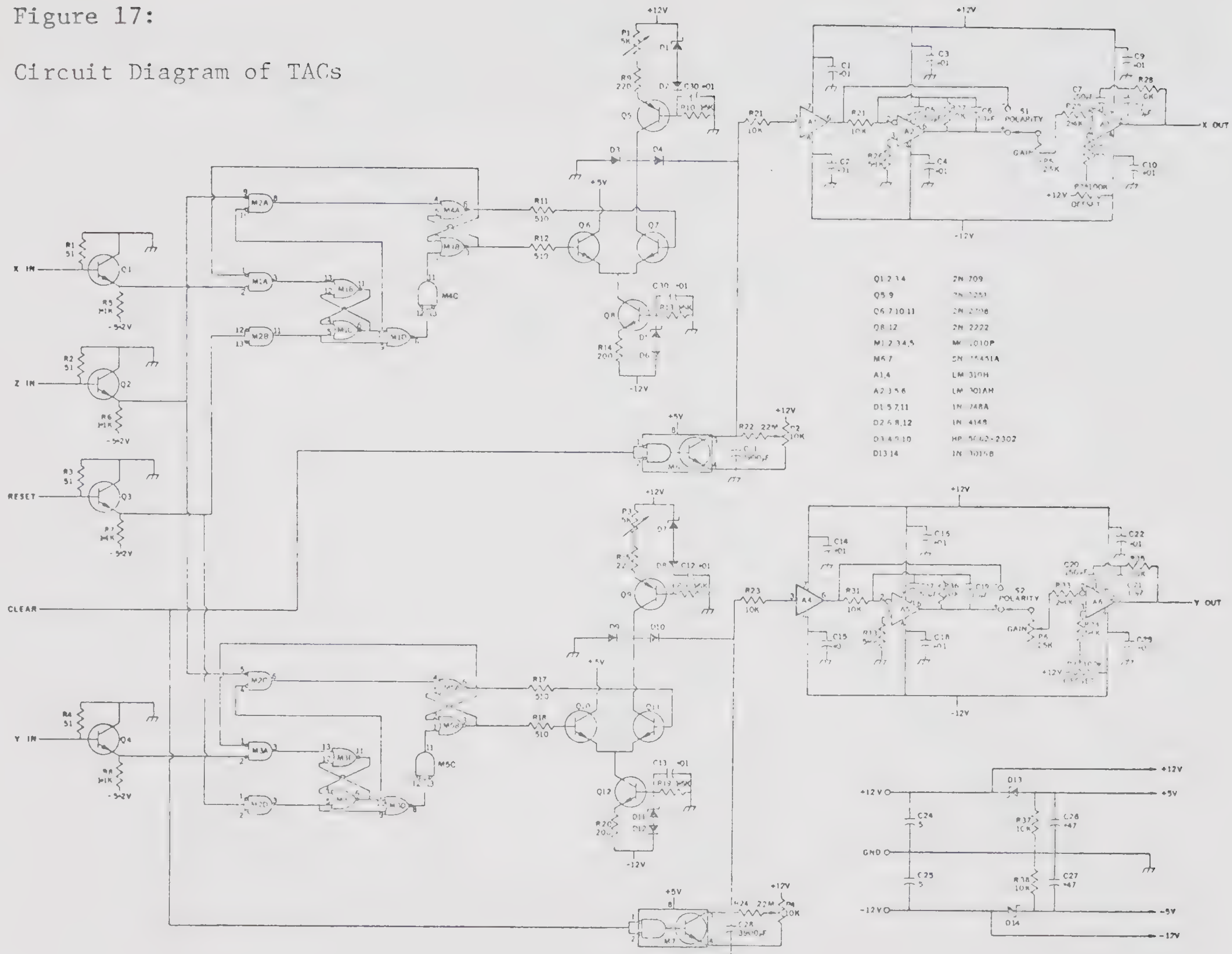

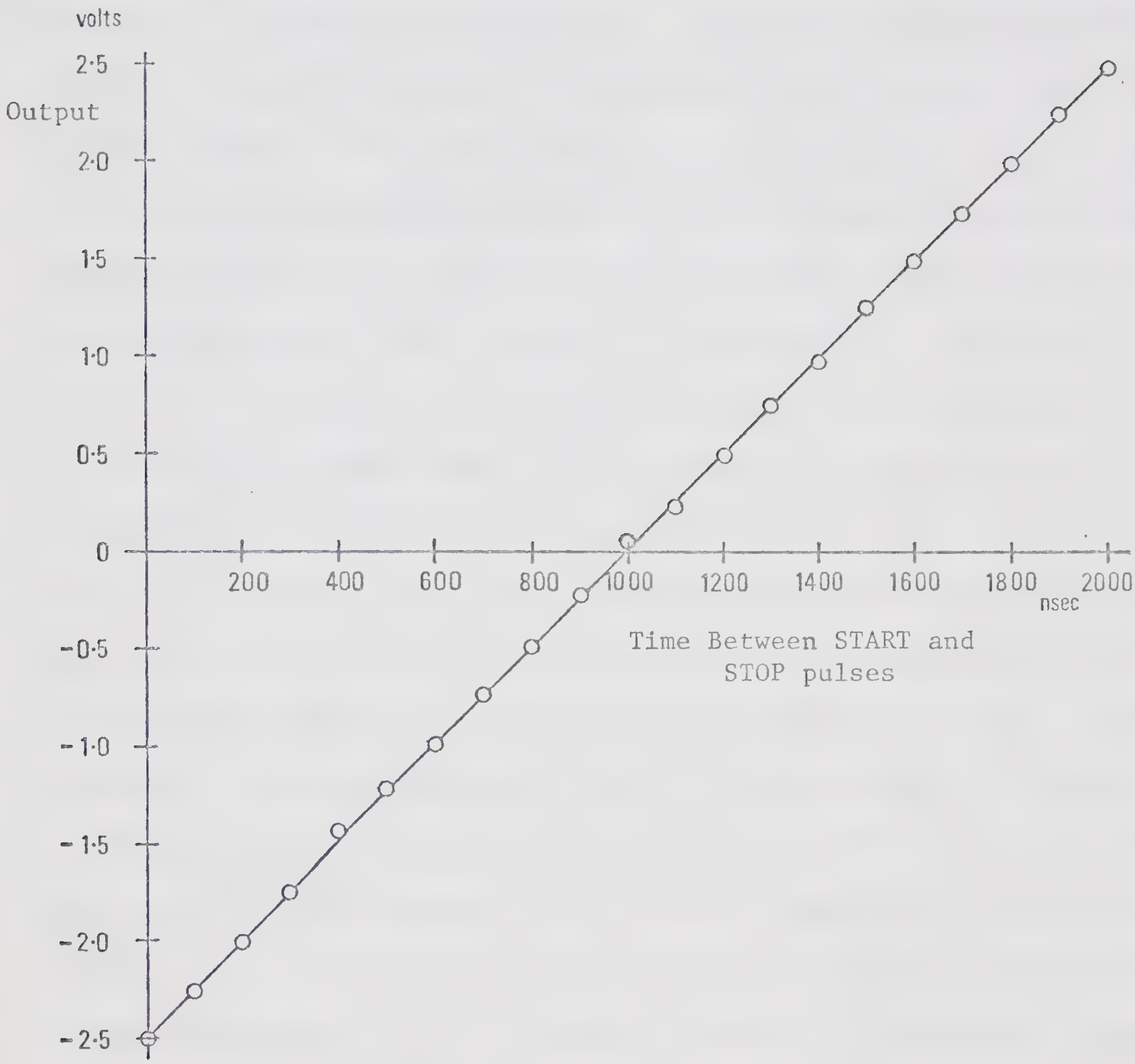


Figure 18: Linearity of TACs

identical, only the former will be described.

Gate M1A ensures that no X pulse can stop the TAC before a Z pulse has started it. Gate M2A ensures that once stopped, the TAC cannot be restarted until a RESET pulse has been received. If these criteria are satisfied, on receipt of a Z pulse the latch formed by M4A and M4B is set, and the collector of Q7 rises. This switches on the current from current-source Q5 and allows it to charge capacitor C11. When an X pulse is received, the latch is reset and the current is switched off. The voltage accumulated by the capacitor is amplified and passed to the output through op-amps A1, A2, A3. The input impedance of these amplifiers is high, so that the voltage on the capacitor can be "held" for several milliseconds. The gain and offset of the output voltage can be varied by P5 and P7 respectively. Switch S1 dictates whether the output will be positive or negative. When the output voltage is no longer required, a CLEAR pulse discharges C11 and the output voltage returns to the "zero" value determined by the offset. Figure 18 shows the output voltage of the TACs as a function of the elapsed time between "start" and "stop" pulses. The offset and gain have been adjusted to make the voltage range compatible with the A/D converter.

### 4.3.3 The System Controller

The System Controller acts as a supervisor for the

elements of the read-out system and provides the communication with the computer. It decides whether the voltages accumulated by the TACs can be used to reconstruct the position vector of a genuine positron annihilation: if so, it instructs the computer to sample and digitize. If not, it sends CLEAR pulses to return the output of the TACs to their "zero" value, and RESET pulses to enable them to collect further data.

After an invalid event, the RESET pulse must not be sent until all data from that event have been collected. For example, it will be known after approximately 100 nanoseconds that a Z pulse from one chamber is not in coincidence with a Z pulse from the other chamber, but the RESET pulses cannot be sent until the corresponding X and Y pulses have been received. Thus the circuit was designed to distinguish between the several different types of invalid data that can occur and correctly time the RESET pulse for each. The varicus possibilities are outlined below (refer to Figure 19):

(a) No Coincidence: When a Z pulse from either chamber is received, monostable multivibrator M14A is triggered. If a Z1 pulse is received without an accompanying Z2 pulse, it will reset after a "resolving time" of the order of 100 nanoseconds has elapsed, setting latch M24A,B. If X1 and Y1 pulses subsequently arrive before a Z2 pulse is detected, M21A goes low as soon as X1 and Y1 are in, and RESET and CLEAR pulses are generated immediately. If, however, a Z2

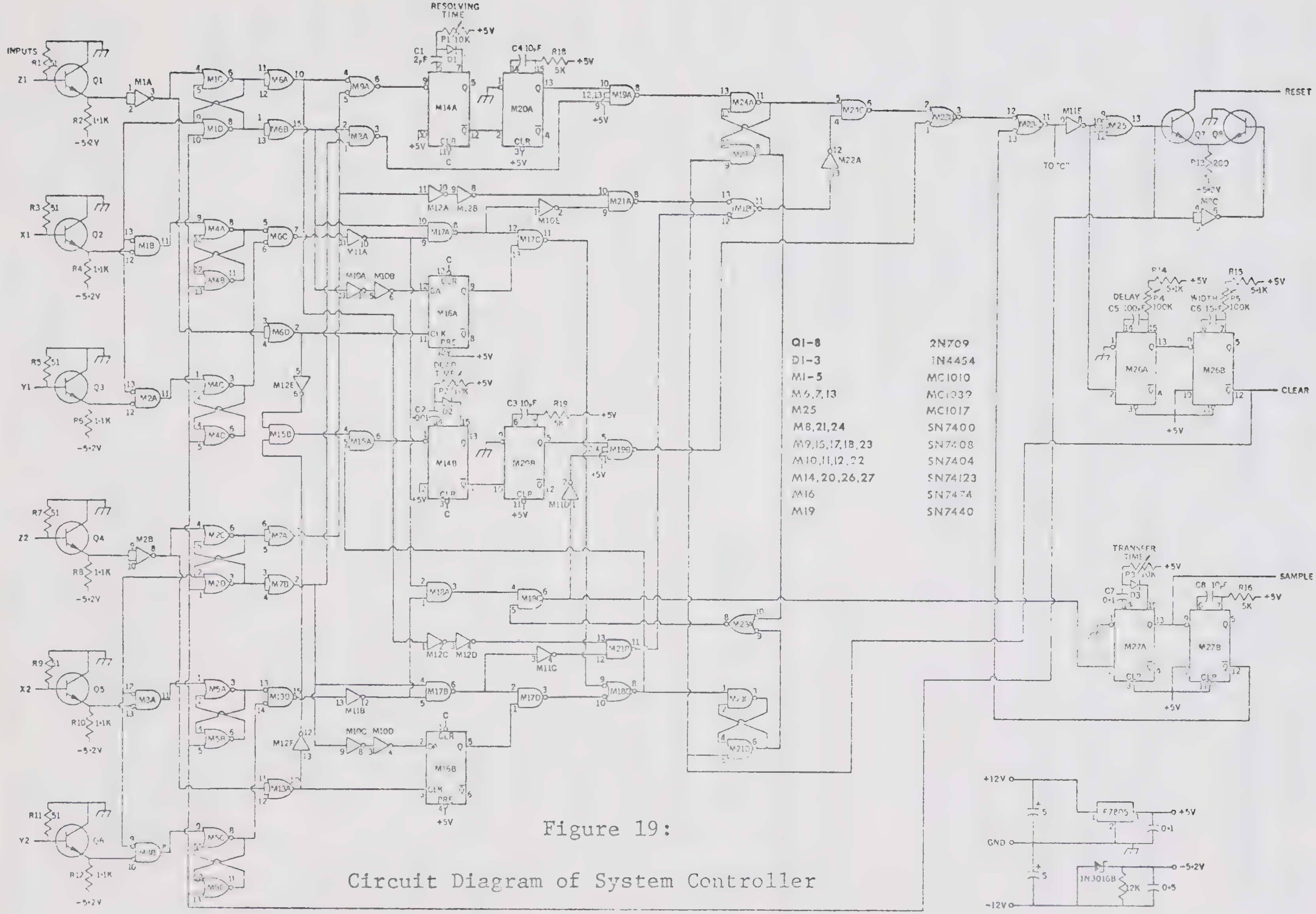


Figure 19:

Circuit Diagram of System Controller

pulse is detected before X1 and Y1 are both in (but after M14A has reset), RESET and CLEAR pulses are generated when M14B resets, after the "dead time" of approximately 2 microseconds.

(b) Missing X or Y Pulse: If Z1 and Z2 pulses arrive within the coincidence resolving time set by M14A, but one of X1, Y1, X2 or Y2 is not detected within the "dead time" of 2 microseconds (the maximum possible time for a pulse to traverse the delay line), RESET and CLEAR pulses are generated when M14B resets.

(c) Pile-up: Shortly after a Z2 pulse is detected, the "DATA" input (pin 2) of M16B goes high. A subsequent Z2 pulse will act as a clock pulse, transfering this high logic level to the output, M16B(5). If X2 and Y2 pulses were not received before the second Z2 pulse, a pile-up condition exists (because it is not known to which Z pulse they correspond) and a pulse is sent to retrigger M14B. Regardless of its status at the time the pile-up was detected, M14B will not reset until a time equal to the dead time has elapsed after the second (retriggering) Z2 pulse. When it finally resets, RESET and CLEAR pulses are generated. The pile-up detection system for Z1 is identical.

(d) True Ccincidence: If Z1 and Z2 arrive within the resolving-time, the "nc ccincidence" pulse from M14A is inhibited at gate M19A. When X1, Y1, X2 and Y2 have all been received, M18C goes high. This inhibits the "dead-time

expired" pulse from M14B, and triggers monostable M27A, sending a SAMPLE command to the computer. A "transfer time" of the order of 100 microseconds is allowed for the computer to digitize and store the data, then M27A resets, sending a short pulse to M23C. M25 translates this pulse to MECL levels and sends a RESET pulse to the TACs. M26B sends a CLEAR pulse after a short delay, which is to compensate for the propagation delay of the reset circuitry of the TACs.

# CHAPTER 5

# RECONSTRUCTION OF IMAGES

## 5.1 Software

An overview of the computer installation in the Biomedical Engineering Laboratory is shown in Figure 20. The CPU is a Hewlett Packard 2100A computer which has a core storage of 16K and a memory cycle time of 980 nanoseconds. Peripherals include an Analogue-to-Digital Converter (HP 5610A) and Pacer (HP 5611A), a 9-track tape drive (HP 7970A), and a graphic display terminal with storage screen (Tektronix 4010-1) and a hard copy unit (Tektronix 4610).

### 5.1.1 Data Acquisition

Continuous on-line data acquisition is effected through a systems program, DATAC. This program responds to a command from the System Controller of the MWPC camera (through the Pacer) by causing the A/D converter to sample and digitize in sequence its first four channels. Two buffers, each of 1024 words, are set up in core to store data from the A/D. These data - a 10-bit binary number from each channel - are left-justified, and 6 bits, including channel identification, are added to each number to make a 16-bit word.

When the first buffer has been filled, subsequent data

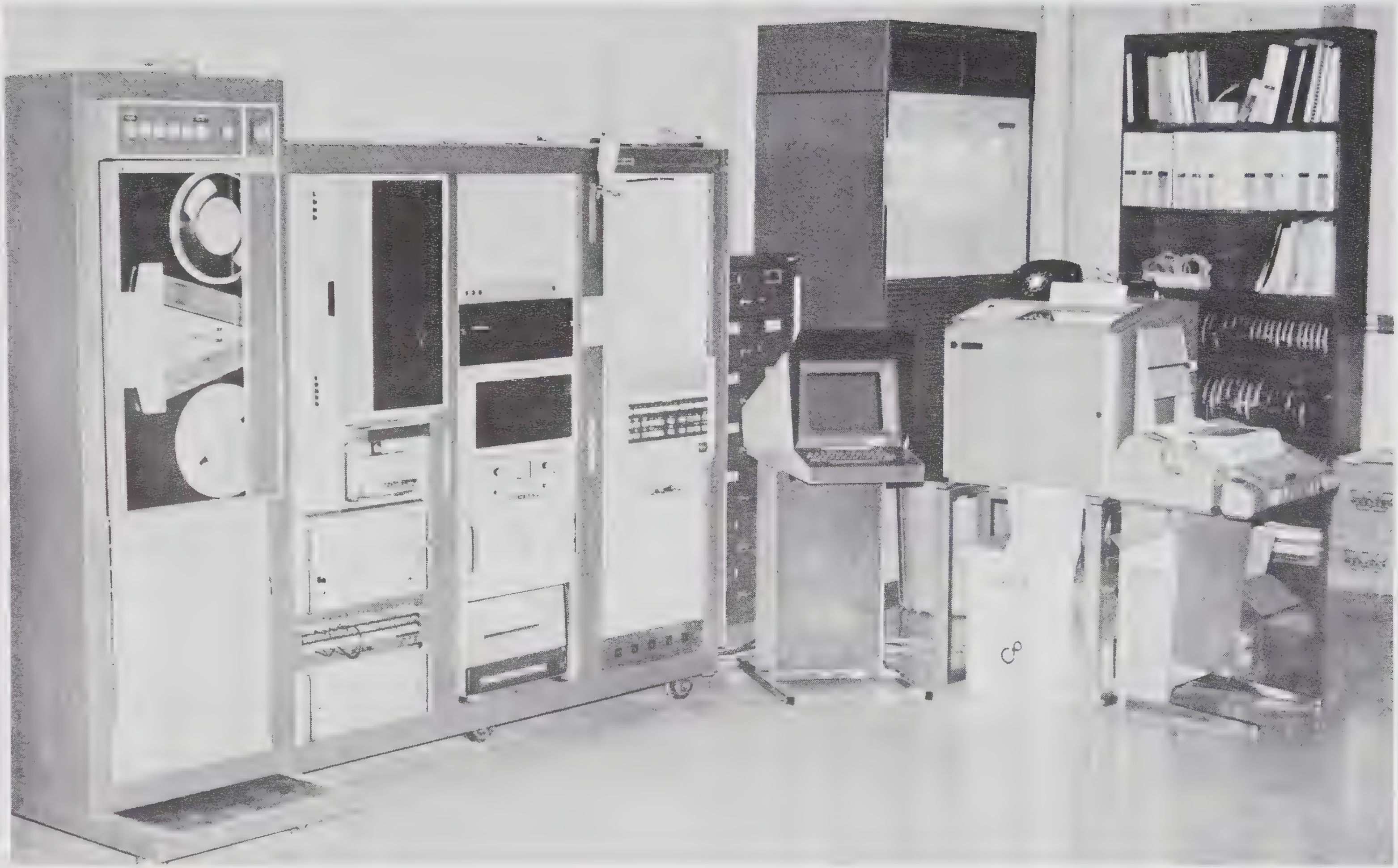

Figure 20: Biomedical Engineering Computer Installation

are stored in the second buffer while the contents of the first are transferred to magnetic tape as one record. Sampling and digitizing are carried out at a frequency of 100 kHz, that is, it takes 10 microseconds to sample and digitize each channel; it takes approximately another 60 microseconds for the program to respond to the Pacer, command each channel of the A/D in sequence, transfer the data to the buffer, and perform general "housekeeping" tasks. However, the rate at which data can be acquired is limited by the time taken to transfer each record to tape, rather than by the 100 microsecond "transfer time" which allows the program to execute after each coincidence has been detected. This limit corresponds to an average rate of 2650 coincidences per second.

### 5.1.2 Image Reconstruction

In order to reconstruct an image, raw data is read from the magnetic tape, processed, and used to create a display. Programs to accomplish this were written in FORTRAN IV and implemented on the HP 2100A. Due to the limited core storage and speed of execution, it was not always possible to use standard library subroutines. In such cases, more economic or faster subroutines were devised. A complete listing of the programs and subroutines appears in the Appendix.

Although the number of events required to obtain a

statistically valid image depends on the complexity of the object and the spatial resolution of the system, in general, of the order of 10,000 events must be recorded. Clearly, amounts of information of this order cannot be stored in core. Two approaches to this storage problem have been investigated, and will be described below. The simplest solution, adopted in the program POINT, is to write each event as a dot in a suitable position on the storage screen as soon as its coordinates have been calculated. In the program GREY, spatial resolution has been traded for contrast to limit the information that must be stored.

(a) POINT: The program POINT uses the subroutine DOSTP (kindly made available by G. Blinston) to locate the desired file on the magnetic tape, and read the file name. The operator then enters parameters defining the separation of the detectors and the desired plane of best focus. Next, the data is read from tape in records of 1024 words. A fixed-point divide by 64 is performed to remove the last six bits of each word, which contain the A/D channel identification. The data is then reduced to provide two coordinates for each of 256 events. These coordinates are converted to screen units and the subroutine DOT is called, for each event, to write a dot on the screen at the appropriate position. Finally, BOX is called to enclose the display with labelled axes.

This program provides a useful overview of the data, indicating areas of the display deserving closer study. Its

chief limitation is the loss of contrast due to the finite resolution of the display screen. In theory there are 1024 x 780 addressable screen points, but in practice, addressing any one of these will cause neighbouring points to be illuminated also. Thus, in regions of moderate count density, the screen reaches the fully written condition and further dots are not visible. This loss of contrast through saturation of the screen is illustrated in Figure 21, which shows a reconstruction of a point source with program POINT. The problem was alleviated by replacing the dot generated in vector plot mode by an alphanumeric period (.), since the hardware of the display terminal is such that this produces a finer dot on the screen. However, this involves making two calls to the Executive module of the system for each dot - the first to position the alphanumeric cursor, the second to write the period - and significantly increases the execution time. The program POINT takes nearly two minutes to process 10,000 events.

(b) GREY: In the program GREY , the approach is to simulate a multi-channel analyser. Each spatial region is represented by an element of an array, and the accumulated count in this region is stored in the corresponding address. This address is in turn represented by a small square on the screen. A "grey scale" is employed to shade this square according to the number of counts occurring in the corresponding region of space. This approach has the advantage of speed: to reproduce a point source from 10,000

Figure 21: Defocusing of Image

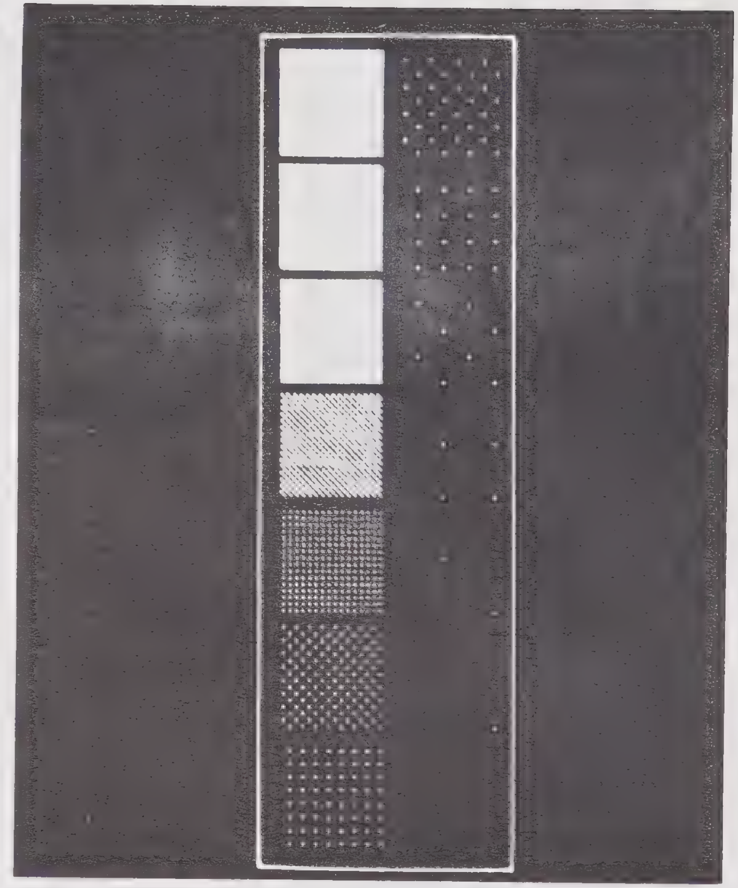

Figure 22: Levels of Grey

Produced by Subroutine SHADE

counts takes 30 seconds. It also produces a more easily interpreted display and makes techniques such as digital smoothing or background subtraction possible.

For convenience, an area of 512 x 512 screen points was chosen to represent the complete field of view of 256 mm square. The largest square array whose side divides 512 which can be stored in core is 64 x 64. For such an array the spatial resolution will be 4 mm, and each of the 64 x 64 small squares drawn on the screen will contain 64 addressable points. As a consequence of the Weber-Fechner law (e.g., Stead 1938), a perceptible increase in darkness requires doubling the number of dots written in these squares. A square containing 64 screen points should accommodate 8 levels of grey, including "white" or blank screen. In practice, on our screen the last three levels are indistinguishable (see Figure 22), and only 6 discrete levels are obtained.

The calling program GREY, like POINT, serves as an interactive link with the operator. In addition to specifying the detector separation and focal plane, the operator can specify a region of interest less than the full field of view. In conjunction with this smaller region of interest he can specify an array smaller than 64 x 64 and thus gain grey levels without losing spatial resolution. As in POINT, the tape is positioned by DOSTP and the data read in records of 1024 words. As each pair of coordinates is calculated, a fast algorithm (L. Friedenberg, private

communication) is used to locate the corresponding element of the stored array. The value of this element is then incremented by one. When all the data have been read in and processed, the maximum and minimum elements of the array are found. The difference between maximum and minimum values is divided by the number of grey levels available to define the range of counts to be assigned to each level of grey. A call to SHADE is then made for each element of the array to produce the correct shade of grey on the screen. Finally, through BOX, a box with labelled edges is drawn around the display.

At this point, control is returned to the operator and he can make a hard copy of the display. Or he can restart the program, choosing a different focal plane or region of interest. A third option uses the system line printer to obtain the values of the elements of any rows or columns of the stored array, from which count profiles may be derived.

## 5.2 Images of Simple Objects

The images of some simple objects, as obtained with the camera, will now be presented and discussed. Different ways of reconstructing the same data from the MWPC camera are illustrated, and some images obtained with the Anger positron camera are included for comparison.

### 5.2.1 Point Source

A point source was constructed from 83 microcuries of $^{22}Na$ embedded in a 2.5 cm cube of plexiglass. Figure 23 shows a grey scale reconstruction of this point source. The point source was situated close to the common axis of the chambers; the distance to the point source from the lower detector was measured directly and used as the focal plane. Each of the 64 x 64 channels corresponds to a spatial region of size 4 mm x 4 mm, and there are 6 distinct grey levels.

Figure 24 shows the same point source, situated off-axis. Figure 25 shows the same data, but with a reduced region of interest. Since only 32 x 32 channels are used, 8 grey levels are available.

### 5.2.2 Line Source

Figure 26 shows a pcint plot of a line source, consisting of 15 microcuries of $^{22}Na$ embedded in an 8.7 cm x 1.3 cm x 1.3 cm plexiglass rod. Figure 27 shows a comparison between images of this line source obtained with the MWPC positron camera and with the Anger positron camera. Figure 28 shows reconstructions of two line sources situated in different planes. The sources, of strength 15 microcuries and 4 microcuries respectively, were placed parallel to the chamber faces but orthogonal to each other. In Figure 28a the plane of best focus passes through the 15 microcurie source; in Figure 28b it passes through the 4

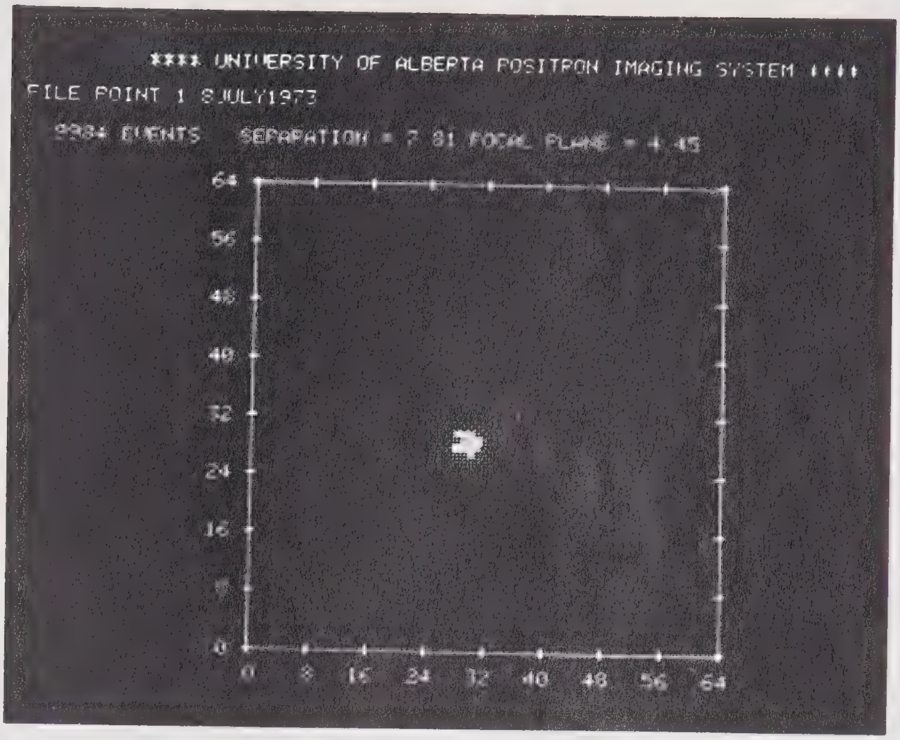


Figure 23: Image of a Point Source (on axis)

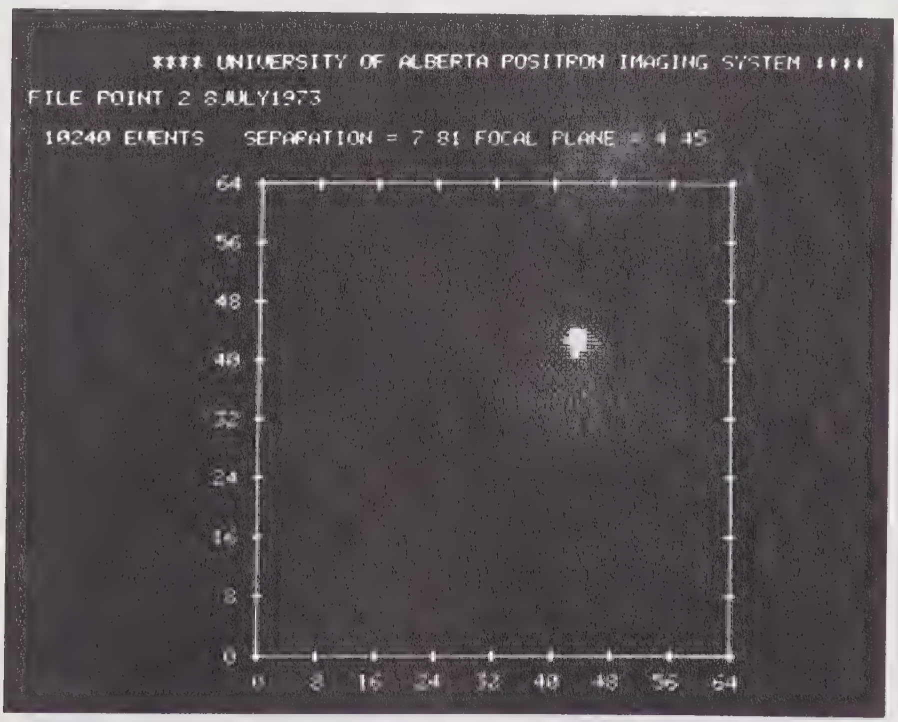


Figure 24: Image of a Point Source (off axis)

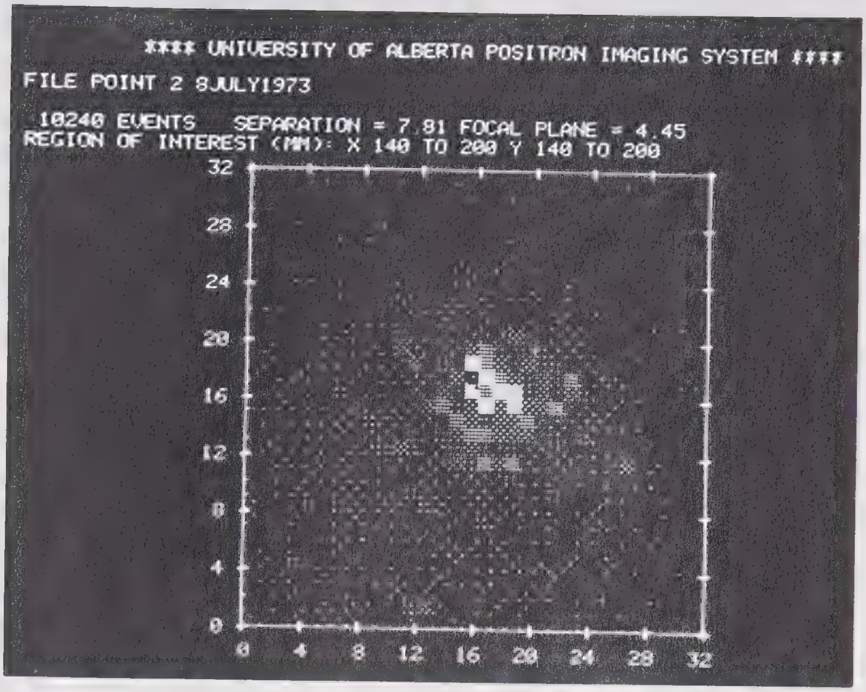


Figure 25: Off Axis Point Source with Reduced Region of Interest

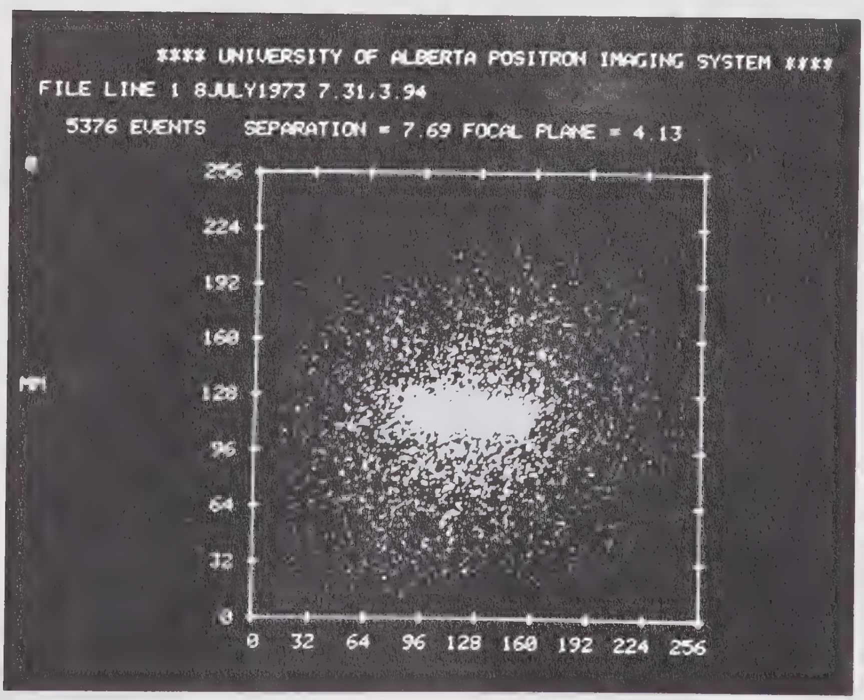


Figure 26: Image of a Line Source (Point Plot)

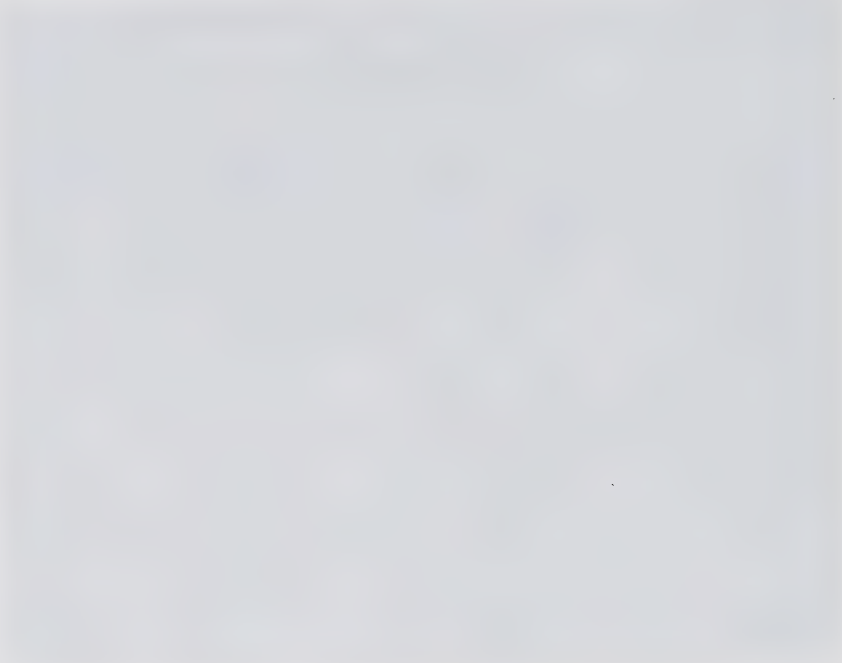

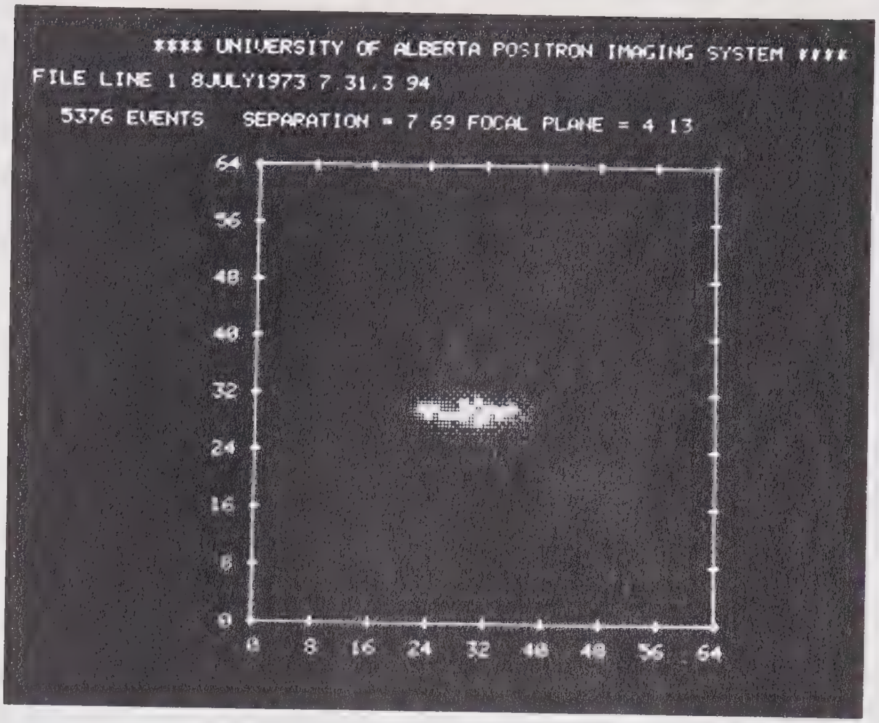


(a) MWPC Positron Camera

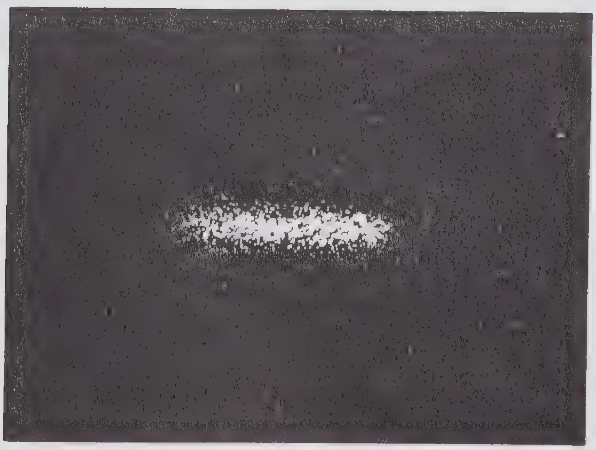

(b) Anger Positron Camera

Figure 27: MWPC and Anger Positron Camera Images of a Line Source

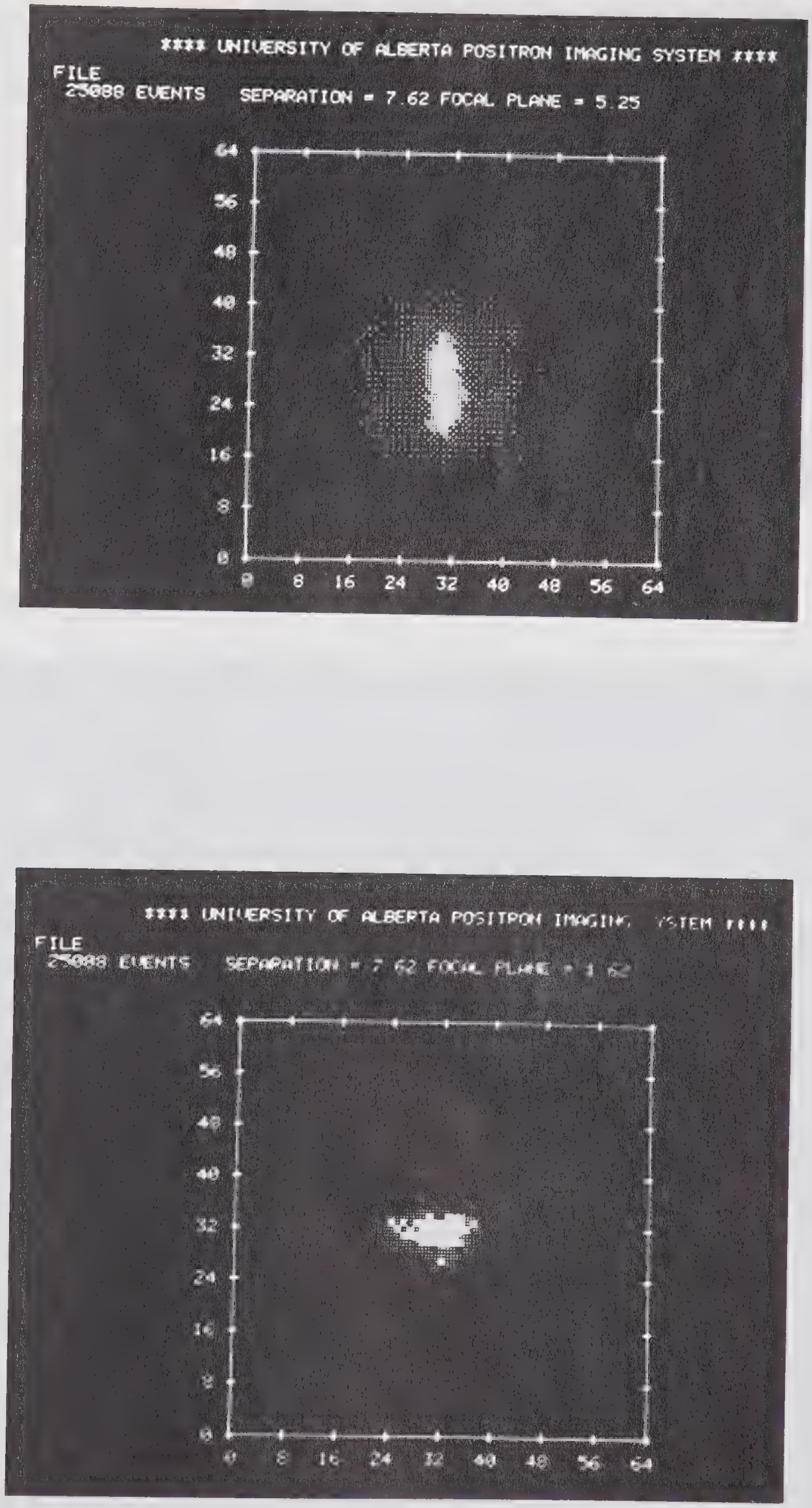


Figure 28: Images of Two Line Sources in Different Planes

Figure 29: Images of a Thyroid Phantom

(a) Anger Positron Camera

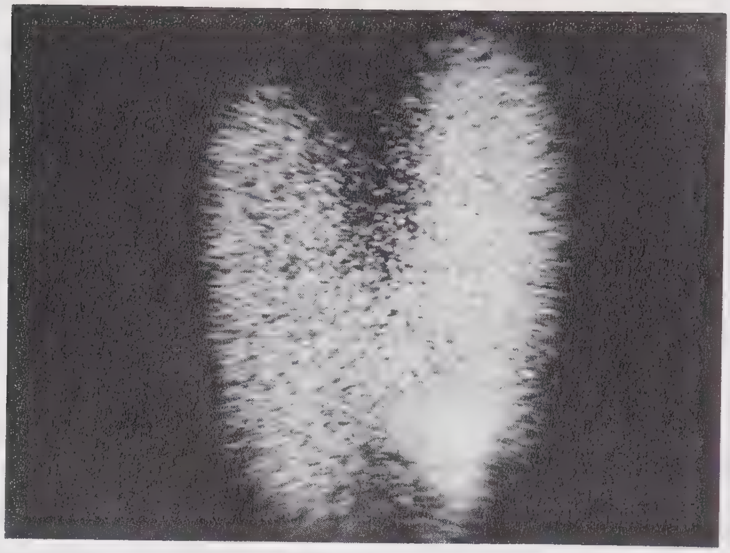

(b) MWPC Positron Camera

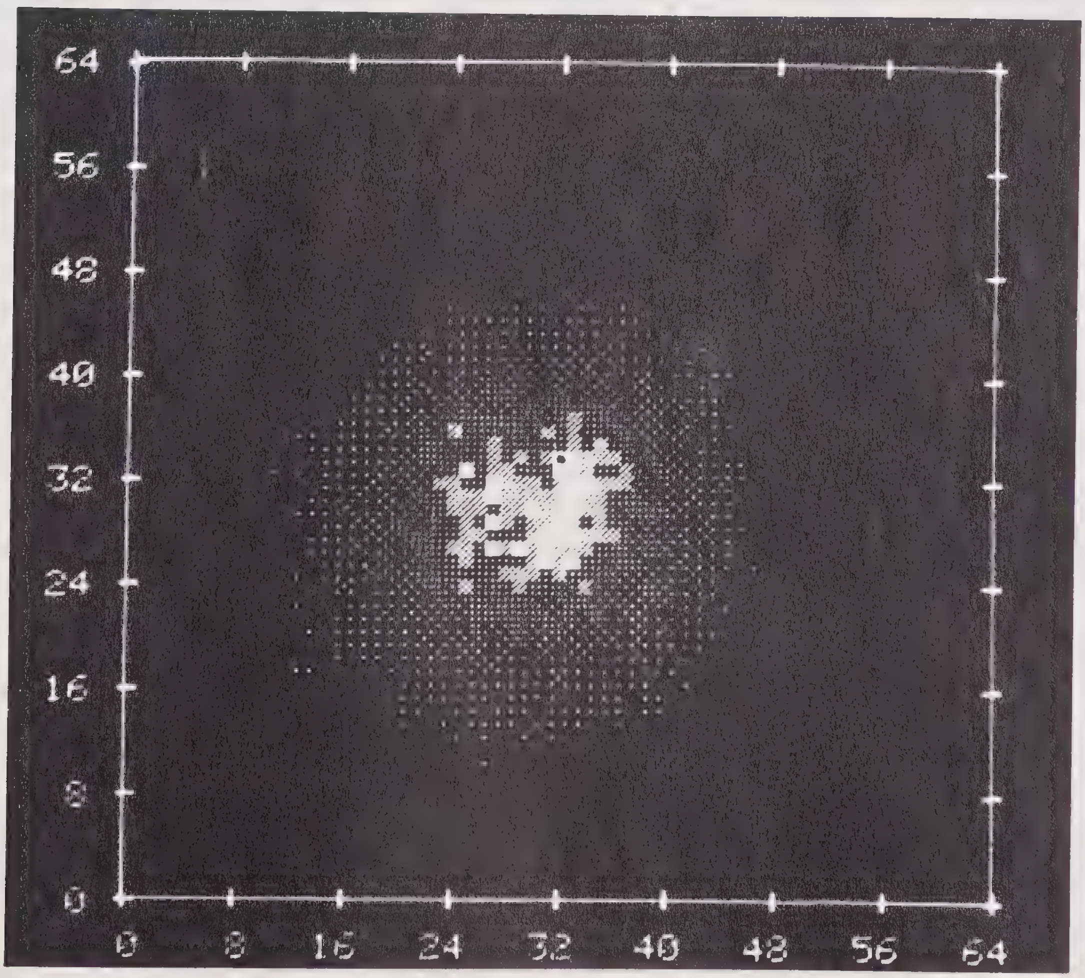

microcurie source.

### 5.2.3 Thyroid Phantom

A commercial thyroid phantom (Picker Nuclear 3062), filled with 20 microcuries of $^{65}Zn$ in 35 cc of water, was used to obtain the images shown in Figure 29. In both views, the plane of best focus passes through the centre of the phantom. Figure 29b, from the MWPC positron camera, clearly shows a "hot" region on the right side of the thyroid, and a "cold" spot on the lower left side. The hot spot is confirmed by Figure 29a, from the Anger positron camera. Unfortunately, the Anger camera was incorrectly focused on this occasion, and the cold spot is less clearly visible.

# CHAPTER 6

# CONCLUSIONS AND SUGGESTIONS FOR FURTHER RESEARCH

## 6.1 System Evaluation

A prototype MWPC positron camera has been constructed, and images of some simple radioactive source distributions have been obtained. The system, however, has a low sensitivity and poor spatial resolution. That these shortcomings can be attributed to certain aspects of the present design and are not inherent in the concept of an MWPC camera is demonstrated below, and suggestions are made by which they may be overcome.

### 6.1.1 Efficiency

With an 83 microcurie pcint source of $^{22}Na$ positioned on axis midway between the chambers, a count rate of 526 per minute was achieved when the chambers were 25 cm apart. From this we deduce that the sensitivity is

$$s = 6.3 \text{ ccunts per minute per microcurie.} \qquad (1)$$

To demonstrate that this low sensitivity is primarily due to the converter foils, an estimate of the efficiencies of the wire chambers (with converter foils) to annihilation radiation was made.

Estimation of the efficiency of the wire chambers to

annihilation radiation is complicated by the fact that most commonly available positron emitters also emit gamma rays, which are difficult to distinguish from annihilation radiation since the system lacks pulse height analysis. To circumvent this difficulty a $^{137}Cs$ source was used, as the energy of the 662 keV caesium gamma ray is sufficiently close to 511 keV to give an estimate of the efficiency.

The activity of the caesium source, as obtained with a standard 3" x 3" NaI(Tl) scintillation spectrometer, was 6.0 microcuries. The count rate was found for each chamber in turn by connecting it in parallel to both sets of inputs to the System Controller. Thus, all counts are regarded as coincidences. Count rates of 142 per second and 125 per second, after correction for room background, were recorded for the two chambers when the geometric factor for each chamber was 0.167. At these low count rates, the effect of pile-up rejection may be neglected. Thus the efficiencies of the chambers for 662 keV gamma rays are 0.46% and 0.41% respectively.

To estimate the sensitivity of a system constructed from detectors with such efficiencies, we calculate the "singles" and "coincidence" count rates expected with a 83 microcurie source of $^{22}Na$. This isotope emits positrons for approximately 90% of its disintegrations, but emits a 1.275 MeV gamma ray at each disintegration. The detection efficiency of these 1.275 MeV gammas can be estimated from the singles count rate, for:

$$S' = (1.8e' + e'')NG\exp(-ST), \tag{2}$$

where $e'$, $e''$ are the efficiencies for 511 keV and 1.275 MeV gamma rays, and $S$, $S'$ are the true and observed singles rates, respectively. The observed mean singles count rate (obtained by connecting each chamber in turn to the System Controller, as described above) was

$$S' = 4180 \text{ per second}, \tag{3}$$

and assuming $ST$ is small,

$$e'' = 0.12\%. \tag{4}$$

The observed coincidence count rate, due to genuine positron annihilations, will be

$$C' = 1.8Ge'^2N\exp(-N'T), \tag{5}$$

where $N'$ is defined as in eqn. (10), Chapter 2. However, some 1.275 MeV gamma rays will be detected coincidentally with the 511 keV annihilation radiation, at the rate

$$C'' = 1.8G^2e'e''N. \tag{6}$$

Thus the expected total coincidence rate (assuming $N'T$ is small) is

$$C' = 987 \text{ per minute} \tag{7}$$

from which the expected sensitivity is

$$S = 11.9 \text{ counts per minute per microcurie.} \tag{8}$$

Thus we conclude that our estimate of efficiency is correct to within better than an order of magnitude.

### 6.1.2 Resolution

To estimate the resolution of the system, a line spread function was obtained. A 15 microcurie line source of $^{22}Na$ was placed parallel to the common X-axis of the two chambers. Since the image reconstruction program GREY represents the X and Y directions by the rows and columns of a stored array, by plotting the values of a suitable column of this array the profile shown in Figure 30c was obtained. The full width at half maximum (FWHM) of this profile is 16 mm, indicating that the spatial resolution of the system is of this order. This is somewhat greater than expected. That this loss of spatial resolution is due to electrons leaving the converter foils and traversing the chamber obliquely is demonstrated by Figures 30a and 30b, which show line spread functions for the wire chambers with a converter foil and with a mylar window, respectively. In each case the source was collimated with two 20 cm x 20 cm x 5 cm lead bricks spaced 1 mm apart, and the line spread function was taken by feeding the output of the appropriate TAC into a multichannel analyser. With the converter foil present, the source used was $^{22}Na$, while with the converter foil replaced

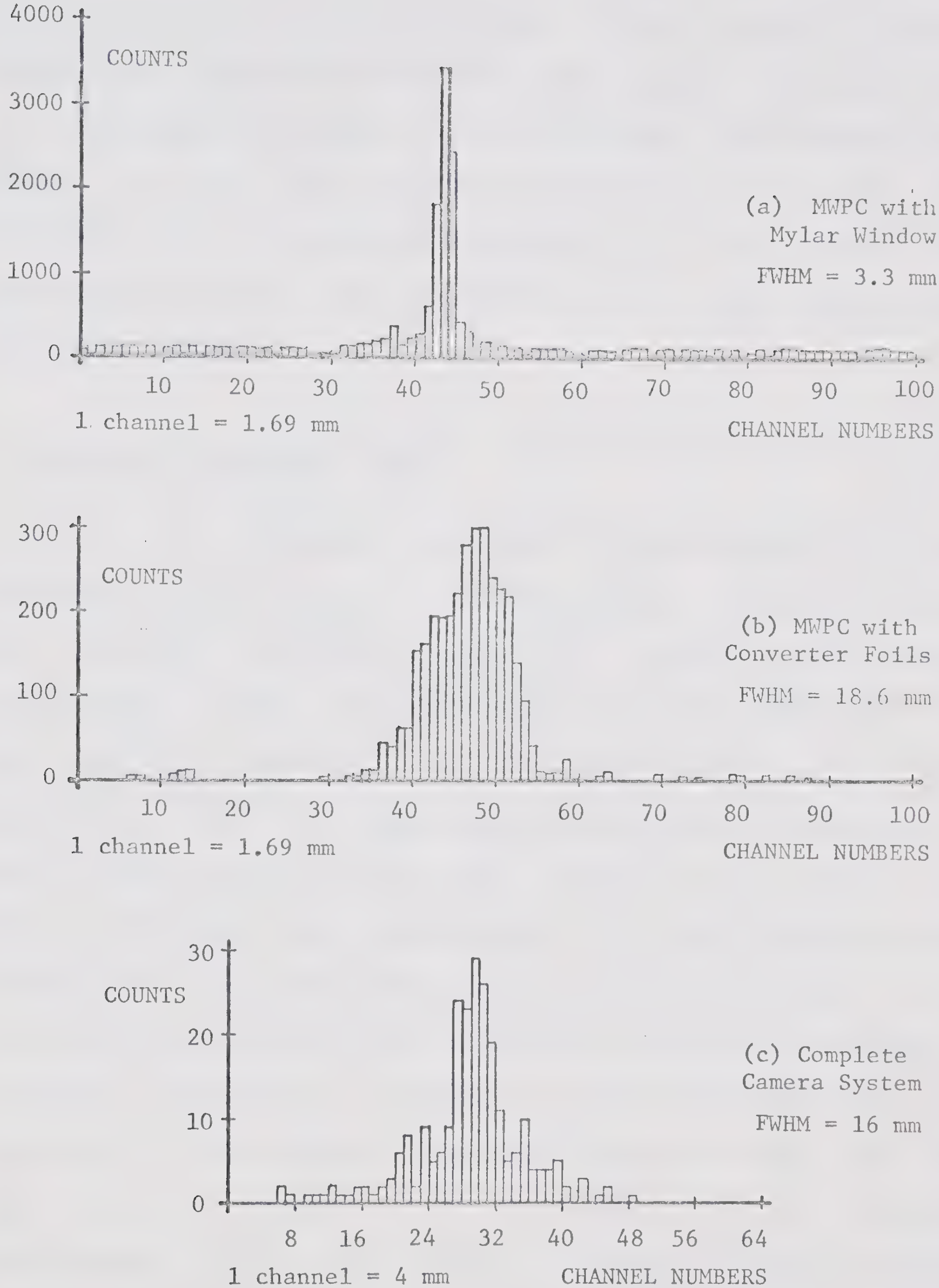


Figure 30: Line Spread Functions from MWPC Camera System

by a mylar window, $^{109}Cd$ was used. A low energy (22keV) isotope was chosen for the latter measurement, to avoid loss of resolution due to long range electrons. The FWHM for the former is 18.6 mm, while for the latter it is 3.3 mm. We conclude that the intrinsic resolution of the chamber is approximately 3 mm, and is degraded for the most part by the converter foils.

## 6.2 Shaped Converter Foils

We are confident that both the resolution and the efficiency can be improved with the shaped converter foils that have been developed by Lim, Chu, Kaufman, Perez-Mendez and Sperinde (1973). They have obtained efficiencies of 4% per foil by increasing the effective surface area of the converters. This is accomplished by forming the lead into a square honey-comb-like structure (Figure 31). Since the field gradients are insufficient to drift out electrons formed deep within the troughs, the walls are divided into two regions separated by an insulating strip, across which a potential difference is applied. With this technique, the resolution of the chambers becomes dependent on the size of the troughs. Troughs 2 mm x 2 mm x 5 mm have been constructed, and the construction of smaller troughs should be feasible. For the 2 mm x 2 mm x 5 mm troughs reported, one would expect a FWHM of about 6 mm.

A drawback of this technique is that the troughs

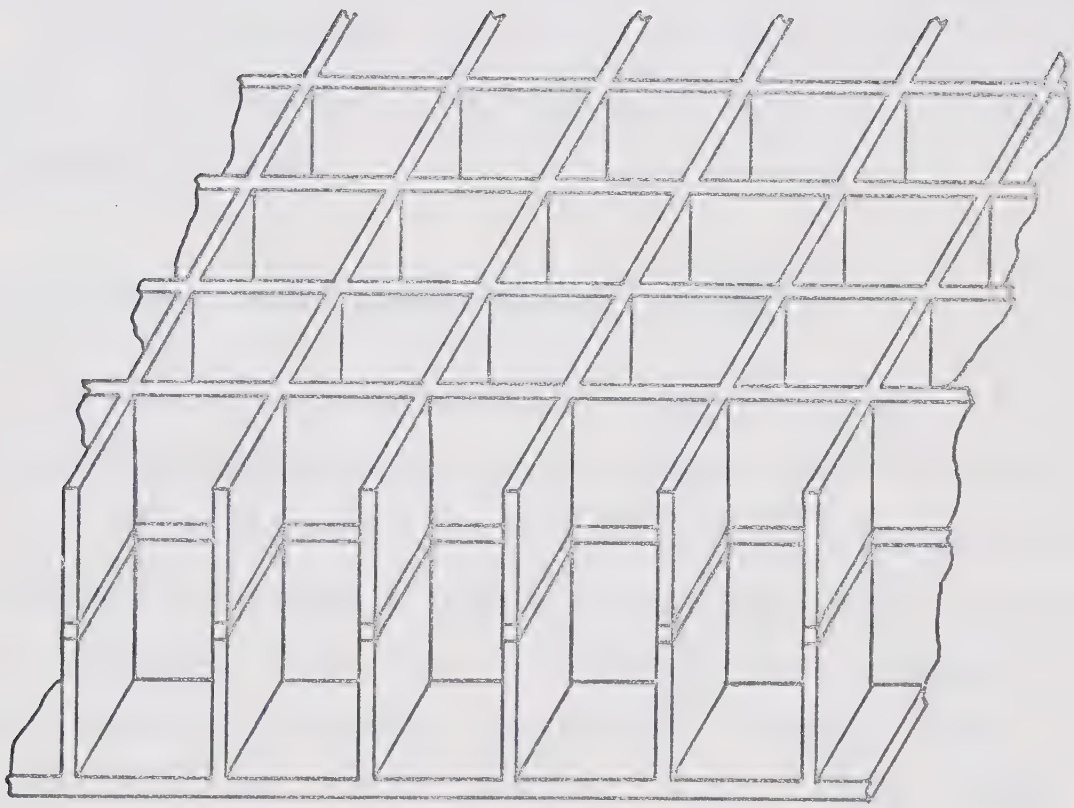

Figure 31: Shaped Converter Foils

(After Lim, Chu, Kaufman, Perez-Mendez and Sperinde 1973)

increase the spread in the transit time of electrons drawn to the anode, degrading the time resolution of the chambers. In a positron imaging system, this will cause a degradation of the signal-to-noise ratio. However, with suitable gas mixtures and drift fields, a time spread of less than 200 nanoseconds FWHM has been reported for the foils described. It may be possible to further decrease this by decreasing the chamber thickness and wire spacing, lowering the pressure, or reducing the effective volume by adding electronegative gases.

## 6.3 Pressurized and Liquid Filled Chambers

A slight improvement to the spatial resolution would be expected by replacing the argon chamber gas by xenon. The use of a gas at higher than atmospheric pressure will also alleviate the loss of spatial resolution due to long range electrons from the converter foils traversing the chamber obliquely. However, experiments recently reported by Atac and Lach (1970) and by Binon, Bobyr, Duteil, Gouanere, Hugon, Spighel and Stroot (1971) indicate that the time resolution is rapidly degraded as the pressure is increased. For the proportional chambers filled with liquid xenon which have been reported by Muller, Derenzo, Smadja, Smith, Smits, Zakland and Alvarez (1971) a resolving time of 200 nanoseconds has been achieved by using a chamber of small effective size (less than 8 mm). These liquid filled

chambers, which have high intrinsic efficiencies, offer spatial resolutions of the order of 30 microns. However, their operation poses severe technical problems and at present their cost is prohibitive.

## 6.4 Software

Increased efficiency and improved spatial resolution should be paralleled by faster data acquisition and better image reconstruction. Faster data acquisition can be achieved by using four fast non-multiplexed A/D converters and writing the result directly onto magnetic tape. Many improvements to the reconstruction programs can be made. One disadvantage of the present software is that programs for data acquisition and for image reconstruction must be run under different operating systems. Through the use of a Real Time Executive system, data acquisition and image reconstruction programs could be run together, and an "instant replay" facility would be available. By storing segments of the programs and arrays on disk and swopping them into core when needed, arrays larger than 64 x 64 could be used. For such large arrays, presentation techniques other than the production of a grey scale on a display screen would be necessary. Tauxe (1967) estimates that for useful reconstructions, at least 20 levels of grey are necessary. Furthermore, these should be in standard deviation increments (Monahan, Beattie and Laughlin 1972).

Such a number of levels can be reproduced on a line-printer (Hutchinson, St Clair Neill and Rimmer 1971). Other possible data presentation techniques are the use of isocount profiles, or "three dimensional" plots.

## 6.5 Conclusion

The concept of a positron camera using MWPCs has been shown to be a viable one. The major shortcomings of the system have been isolated and we are confident that with the inclusion of converter foils of improved design, these can be overcome. Through minor improvements to the system on the basis of the experience gained, a camera with sufficient reliability and simplicity of operation for regular clinical usage can be evolved, which together with more sophisticated software will make the system a realistic alternative to presently available positron cameras.

REFERENCES

ANGER, H.O., 1958, Scintillation Camera, Rev. Sci. Instrum., 29, 27.

ANGER, H.O., and ROSENTHAL, D.J., 1959, Scintillation Camera and Positron Camera, in Proc. Med. Radicisotope Scanning (Vienna: IAEA), p. 59.

ATAC, M., and LACH, J., 1970, High Spatial Resolution Proportional Chambers, Nucl. Instrum. Meth., 86, 173.

BINON, F., BOBYR, V.V., DUTEIL, P., GOUANERE, M., HUGON, L., SPIGHEL, M., and STROOT, J.P., 1971, Low Pressure Multiwire Proportional Chambers with High Time Resolution for Strongly Ionizing Particles, Nucl. Instrum. Meth., 94, 27.

BOUCLIER, R., CHARPAK, G., DIMCOVSKI, Z., FISCHER, G., SAULI, F., COIGNET, G., and FLUGGE, G., 1970, Investigation of Some Properties of Multiwire Proportional Chambers, Nucl. Instrum. Meth., 88, 149.

BROWNELL, H.J., and SHALEK, R.J., 1970, Nuclear Physics in Medicine, Physics Today, 23,32.

BROWNELL, G.L., and SWEET, W.H., 1953, Localization of Brain Tumours with Positron Emitters, Nucleonics, 11, 40.

BURNHAM, C.A., ARONOW, S., and BROWNELL, G.L., 1967, New Instrumentation in Positron Scanning, in Radioactive Isotopes in the Location of Tumours, ed. V.R. Mc Cready (Vienna: IAEA), p. 16.

CHARPAK, G., 1970, Evolution of the Automatic Spark Chambers, Ann. Rev. Nucl. Sci., 20, 221.

CHARPAK, G., 1970, Evolution of the Automatic Spark Chamber, Ann. Rev. Nucl. Sci., 20, 221

CHARPAK, G., BOUCLIER, R., BRESSANI, T., FAVIER, J., and ZUPANCIC, C., 1968a, The Use of Multiwire Proportional Counters to Select and Localize Charged Particles, Nucl. Instrum. Meth., 62, 262.

CHARPAK, G., BOUCLIER, R., BRESSANI, T., FAVIER, J., and ZUPANCIC, C., 1968b, Some Read-out Systems for Proportional Multiwire Chambers, Nucl. Instrum. Meth., 65, 217.

CHATTERJEE, T.K., DRAPER, L., HOWELLS, M.R., and OSMAN, P.E., 1973, An Efficient Spark Chamber Detector for Annihilation Radiation, J. Phys. E: Sci. Instrum., 6, 135.

CUNITZ, H., SIPPACH, W., and DIEPERINK, J., 1971, A 5000 Wire Proportional Chamber Readout System for a Large-Aperture Magnet Spectrometer, Nucl. Instrum. Meth., 91, 211.

DELANEY, C.F.G., 1969, Electronics for the Physicist (Harmondsworth: Penguin Books), p. 161.

FREEDMAN, G.S., 1970, Tomography with a Gamma Camera, J. Nucl. Med., 11, 602.

FUZESY, R.J., JAROS, J., KAUFMAN, L., MERRINER, J., PARKER, S., PEREZ-MENDEZ, V., and REDNER, S., 1972, A Gas Mixture for Multiwire Proportional Chambers with High Proportional Gain, Nucl. Instrum. Meth., 100, 267.

GEDCKE, D.A., and McDONALD, W.J., 1967, A Constant Fraction of Pulse Height Trigger for Optimum Time Resolution, Nucl. Instrum. Meth., 55, 377.

GROVE, R., KO, I., LESKOVAR, B., and PEREZ-MENDEZ, V., 1972, Phase Compensated Electromagnetic Delay Lines for Wire Chamber Readout, Nucl. Instrum. Meth., 99, 381.

GROVE, R., PEREZ-MENDEZ, V., and SPERINDE, J., 1973, Improved Delay Lines for Proportional Wire Chamber Readout, Nucl. Instrum. Meth., 106, 407.

GRUNBERG, C., COHEN, L., and MATHIEU, L., 1970, Multiwire Proportional and Semiproportional Counter with a Variable Sensitive Volume, Nucl. Instrum. Meth., 78, 102.

HUTCHINSON, F., ST. CLAIR NEILL, G.D., and RIMMER, A.R., 1971, Lineprinter Display of Digital Scintiscans, Am. J. Roentg., 113, 755.

KAPLAN, S.N., KAUFMAN, L., PEREZ-MENDEZ, V., and VALENTINE, K., 1973, Multiwire Proportional Chambers for Biomedical Application, Nucl. Instrum. Meth., 106, 397.

KAUFMAN, L., PEREZ-MENDEZ, V., POWELL, M., and STOKER, G., 1972, Laminographic Excitation Camera for Thyroid Imaging, IEEE Trans. Nucl. Sci., 19, 46.

KAUFMAN, L., PEREZ-MENDEZ, V., SHAMES, D., and STOKER, G., 1972, A Multi-wire Proportional Chamber for Nuclear Medicine Applications, IEEE Trans. Nucl. Sci., 19, 169.

KELLERSHOHN, C., DESGREZ, A., and LANSIART, A., 1964, Deux nouveaux types, de detecteur pour camera a rayons X ou gamma, in Proc. Symp. Med. Radioisotope Scanning (Vienna: IAEA), Vol. 1, p. 333.

KUHL, D.E., 1967, A Clinical Radioisotope Scanner for Cylindrical and Section Scanning, in Medical Radioisotope Scanning, Vol. 1 (Vienna: IAEA), p. 273.

LANSIART, A., and LELOUP, J., 1963, Chambre a etincelle autodeclenchee, Congres Electronique Nucleaire, OCDE, p. 83.

LIM, C.B., CHU, D., KAUFMAN, L., PEREZ-MENDEZ, V., and SPERINDE, J., 1973, Characteristics of Multiwire Proportional Chambers for Positron Imaging, to be published in IEEE Trans. Nucl. Sci.

McCREADY, V.R., PARKER, R.P., GUNNERSEN, E.M., ELLIS, R., MOSS, E., GORE, W.G., and BELL, J., 1971, Clinical Tests on a Prototype Semiconductor Gamma-Camera, Br. J. Radiol., 44, 58.

MALLARD, J.R., 1967, Principles of Scanning and Current Physical Problems, in Radioactive Isotopes in the Location of Tumours, ed. V.R. McCready (New York: Grune and Stratton), p. 1.

MONAHAN, W.G., BEATTIE, J.W., and LAUGHLIN, J.S., 1972, Positron Mode of the Total Organ Kinetic Imaging Monitor, Phys. Med. Biol., 17, 503.

MULLER, R.A., DERENZO, S.E., SMADJA, G., SMITH, D.B., SMITS, R.G., ZAKLAND, H., and ALVAREZ, L.W., 1971, A Liquid-Filled Proportional Counter, Phys. Rev. Letters, 27, 532.

NUCLEAR CHICAGO CORPORATION, 1967, Instruction Manual: Pho/Gamma III Scintillation Camera System Model 6403, publication no. 714160.

ORMAN, P.R., 1963, A Synchronising Discriminator for Scintillation Counter Pulses, Nucl. Instrum. Meth. 21, 121.

PAGES, R., 1970, Electronics Circuits Associated to multiwire Proportional Chambers, Nucl. Instrum.

Meth., 85, 211.

PARKER, S., JONES, R., KADYK, J., STEVENSON, M.L., KATSURA, T., PETERSON, V.Z., and YOUNT, D., 1971, Multiwire Proporticnal Chambers with Uniform Gain, Nucl. Instrum. Meth., 97, 181.

RINDI, A., PEREZ-MENDEZ, V., and WALLACE, R., 1970, Delay-line Readout for Proportional Chambers, Nucl. Instrum. Meth., 77, 325.

ROSSI, B., and STAUB, H., 1949, Ionization Chambers and Counters (New York: McGraw-Hill), p. 97.

SHEINGOLD, D.H., 1972, ed., Analog-Digital Conversion Handbook (Massachussets: Analog Devices, Inc).

STEAD, G., 1938, Elementary Physics (London: Churchill), p. 226.

TAUXE, W.N., 1967, Tumour Localisation by Scintiscanning Technique: Digital Computer Processing, in Radioactive Isotopes in the Location of Tumours, ed. V. R. McCready (New York: Grune and Stratton), p. 63.

TER-POGOSSIAN, M.M., KASTNER, J., and VEST, T.B., 1963, Autoflourography of the Thyroid Gland by means of Image Amplification, Radiology, 81, 984.

TRIPPE, T., 1969, Minimum Tension Required for Charpak Chamber Wires, CERN Nuclear Physics Internal Report 69, 18.

VALENTINE, K., KAPLAN, S., KAUFMAN, L., and PEREZ-MENDEZ, V., 1972, The Adaptation of Multi-Wire Proportional Chambers with Delay-Line Readouts for Neutron Radiographic Imaging, IEEE Trans. Nucl. Sci., 19, 374.

WATT, D.E., and RAMSDEN, D., 1964, High Sensitivity Counting Techniques (New York: Macmillan), p. 130.

WRENN, F.W. Jr., GOOD, M.I., and HANDLER, P., 1951, The use of positron-emitting radioisotopes for the localization of brain tumours, Science 113, 525.

WYNCHANK, S., 1970, Uniform Tension in a Plane Array of Thin Parallel Wires, Nucl. Instrum. Meth., 87, 317.

ZEIDES DES PLANTES, B.G., 1932, Planigraphy, Acta Radiol, May 15.

# APPENDIX

## PROGRAMS AND SUBROUTINES FOR IMAGE RECONSTRUCTION

```
FTN4,L
      PROGRAM POINT
C
C     THIS PROGRAM READS DATA FROM TAPE, PROCESSES THEM
C     TO FIND THE COORDINATES OF EACH EVENT, AND PRODUCES
C     A DOT AT THE CORRESPCNDING SCREEN POSITION
C
      DIMENSION IRAW(1024),LABEL(37),IB(2)
      COMMON IB
C
C     INITIALIZE VARIABLES
      NREC=0
      ID=27040B
C
C     POSITION TAPE, READ FILE NAME
      CALL DOSTP(LABEL)
      DO 3 I=1,37
      IF(LABEL(I).EQ.0)LABEL(I)=2H
    3 CONTINUE
      WRITE(1,102)LABEL
  102 FORMAT(" FILE ",37A2)
C
C     OPERATOR ENTERS PARAMETERS
      WRITE(1,101)
  101 FORMAT(" ENTER SEPERATION AND FOCAL PLANE      ")
      READ(1,*)B,A
      CALL EXEC(3,1)
      WRITE(1,111)
C
C     READ DATA FROM TAPE
    4 CALL EXEC(1,114B,IRAW,1024)
      IF(IEOF(12))11,20,20
   20 NREC=NREC+1
C
C     REMOVE A/D CHANNEL IDENTIFIER
      DO 5 I=1,1024
    5 IRAW(I)=IRAW(I)/64
C
C     CALCULATE COORDINATES CF EVENT
      DO 6 I=1,1024,4
      X=FLOAT(IRAW(I+2))+A/B*FLOAT(IRAW(I)-IRAW(I+2))
      Y=FLOAT(IRAW(I+3))+A/B*FLOAT(IRAW(I+1)-IRAW(I+3))
C
C     DRAW DOT ON SCREEN
      IB(1)=0.50*(X+512.)+256.
```

```
      IB(2)=0.50*(Y+512.)+134.
      CALL DOT(IB)
    6 CONTINUE
      GO TO 4
   11 CONTINUE
  111 FORMAT(10X,"**** UNIVERSITY OF ALBERTA POSITRON
     1IMAGING SYSTEM ****",//)
      NEV=NREC*256
C
C     DRAW BOX AROUND DISPLAY AND ADD SCALES
      CALL BOX(256,256,1)
C
C     WRITE RELEVANT DATA ABOVE DISPLAY
      IB(1)=0
      IB(2)=730
      CALL EXEC(2,3001B,IB,1)
      WRITE(1,102)LABEL
      WRITE(1,100)NEV,B,A
  100 FORMAT(" ",I6," EVENTS",3X,"SEPARATION =",F5.2,"
     1FOCAL PLANE =",F5.2)
      END
      END$
```

```
FTN4,L
      PROGRAM GREY
C
C     THIS PROGRAM READS DATA FROM TAPE, PROCESSES THEM
C     TO FIND THE NUMBER OF EVENTS OCCURRING IN A GIVEN
C     SPATIAL REGION, AND STCRES THIS NUMBER IN THE
C     CORRESPONDING ELEMENT OF AN ARRAY.  A DISPLAY IS
C     PRODUCED, REPRESENTING THIS NUMBER BY A SUITABLE
C     SHADE OF GREY.
C
      DIMENSION IRAW(1024),IB(2)
      DIMENSION MATR(64,64),LABEL(37),IQS(1),IRS(1),ISS(1)
      COMMON IB
C
C     INITIALIZE VARIABLES
   28 ITEST=0
      MAX=(-32768)
      MIN=32767
      NREC=0
      DO 2 I=1,64
      DO 2 J=1,64
    2 MATR(I,J)=0
C
C     POSITION TAPE, READ FILE NAME
      CALL DOSTP(LABEL)
      DO 3 I=1,37
      IF(LABEL(I).EQ.0)LABEL(I)=2H
```

```
    3 CONTINUE
      WRITE(1,102)LABEL
  102 FORMAT(" FILE ",37A2)
C
C     OPERATOR ENTERS PARAMETERS AND INSTRUCTIONS
      WRITE(1,101)
  101 FORMAT("ENTER SEPARATION AND FOCAL PLANE    ")
      READ(1,*)B,A
      WRITE(1,107)
  107 FORMAT("REGION OF INTEREST OPTION?    ")
      READ(1,108)IQS
  108 FORMAT(1A2)
      IF(IQS.NE.2HYE)GO TO 25
      ITEST=1
      WRITE(1,109)
  109 FORMAT("X  (MM)   ")
      READ(1,*)IX1,IX2
      WRITE(1,110)
  110 FORMAT("Y  (MM)   ")
      READ(1,*)IY1,IY2
      GO TO 24
   25 IX1=0
      IX2=256
      IY1=0
      IY2=256
   24 IRX1=4*IX1-512
      IRX2=4*IX2-512
      IRY1=4*IY1-512
      IRY2=4*IY2-512
      WRITE(1,105)
  105 FORMAT("ARRAY OF SIDE 64 32 16 OR 8?    ")
      READ(1,*)NSIZE
      MG=512/NSIZE
      IF(MG.EQ.8)NGREY=6
      IF(MG.EQ.16)NGREY=8
      IF(MG.EQ.32)NGREY=10
      IF(MG.EQ.64)NGREY=12
      WRITE(1,106)NGREY
  106 FORMAT(I2," GREY LEVELS")
C
C     READ DATA FRCM TAPE
    4 CALL EXEC(1,114B,IRAW,1024)
      IF(IEOF(12))11,20,20
   20 NREC=NREC+1
C
C     REMOVE A/D CHANNEL IDENTIFIER
      DO 5 I=1,1024
    5 IRAW(I)=IRAW(I)/64
C
C     CALCULATE COORDINATES OF EVENT
      DO 6 I=1,1024,4
      X=FLOAT(IRAW(I+2))+A/B*FLOAT(IRAW(I)-IRAW(I+2))
      Y=FLOAT(IRAW(I+3))+A/B*FLOAT(IRAW(I+1)-IRAW(I+3))
```

```
C
C     COMPARE TO REGION OF INTEREST
      IF(X.LT.IRX1)GO TO 6
      IF(X.GT.IRX2)GO TO 6
      IF(Y.LT.IRY1)GO TO 6
      IF(Y.GT.IRY2)GO TO 6
C
C     INCREASE CORRESPONDING ELEMENT OF ARRAY BY ONE
      LX=FLOAT(NSIZE)*(X-FLOAT(IRX1))/FLOAT(IRX2-IRX1)+1
      LY=FLOAT(NSIZE)*(Y-FLOAT(IRY1))/FLOAT(IRY2-IRY1)+1
      MATR(LX,LY)=MATR(LX,LY)+1
    6 CONTINUE
      GO TO 4
   11 CONTINUE
      CALL EXEC(3,1)
      WRITE(1,111)
C
C     FIND MAXIMUM AND MINIMUM OF VALUES STORED IN ARRAY
      DO 19 I=1,NSIZE
      DO 19 J=1,NSIZE
      IF(MATR(I,J).GT.MAX)MAX=MATR(I,J)
      IF (MATR(I,J).LT.MIN)MIN=MATR(I,J)
   19 CONTINUE
C
C     ASSIGN CORRESPONDING GREY LEVEL
      DO 13 I=1,NSIZE
      DO 13 J=1,NSIZE
      LG=FLOAT(NGREY)*FLOAT(MATR(I,J)-MIN)/FLOAT(MAX-MIN)+1
C
C     PRODUCE DISPLAY
      MX=MG*(I-1)+256
      MY=MG*(J-1)+134
      CALL SHADE(MX,MY,MG,LG)
   13 CONTINUE
   27 NEV=NREC*256
C
C     DRAW BOX AROUND DISPLAY AND ADD SCALE
      CALL BOX(NSIZE,NSIZE,0)
  111 FORMAT(10X,"**** UNIVERSITY OF ALBERTA POSITRON
     1IMAGING SYSTEM ****",//)
C
C     WRITE RELEVANT DATA ABOVE DISPLAY
      IB(1)=0
      IB(2)=730
      CALL EXEC(2,3001B,IB,1)
   34 WRITE(1,102)LABEL
      WRITE(1,100)NEV,B,A
  100 FORMAT(" ",I6," EVENTS",3X,"SEPARATION =",F5.2,"
     1FOCAL PLANE =",F5.2)
      IF(ITEST.EQ.0)GO TO 26
      WRITE(1,112)IX1,IX2,IY1,IY2
  112 FORMAT(" REGION OF INTEREST (MM): X ",I3," TO ",I3,"
     1Y ",I3," TO ",I3)
```

```
   26 CONTINUE
C
C     RESTART, TERMINATE PROGRAM, OR PRODUCE
C     SERIAL PRINT-OUT
   32 READ(1,108)IRS
      IF(IRS.EQ.2HRS)GO TO 28
      IF(IRS.EQ.2HSE)GO TO 29
      STOP
   29 WRITE(1,113)
  113 FORMAT(" SERIAL READ-OUT MODE")
      WRITE(1,116)
  116 FORMAT(" READ-OUT BY ROWS OR COLUMNS?    ")
      READ(1,108)ISS
      WRITE(1,117)
  117 FORMAT(" ROW OR COLUMN NUMBERS?    ")
      READ(1,*)NC1,NC2
      IF(ISS.EQ.2HCO)GO TO 30
      WRITE(6,111)
      WRITE(6,113)
      WRITE(6,102)LABEL
      WRITE(6,100)NEV,B,A
      WRITE(6,112)IX1,IX2,IY1,IY2
C
C     PRINT OUT DESIRED ROW OR COLUMN OF ARRAY
      DO 31 J=NC1,NC2
      WRITE(6,114)J
  114 FORMAT(" ROW NUMBER ",I2)
   31 WRITE(6,115) (MATR(I,J),I=1,NSIZE)
  115 FORMAT(" ",5/,16I5)
      GO TO 32
   30 DO 33 I=NC1,NC2
      WRITE(6,118)I
  118 FORMAT(" COLUMN NUMBER ",I2)
   33 WRITE(6,115) (MATR(I,J),J=1,NSIZE)
      GO TO 32
      END
      END$
```

```
FTN4,L
      SUBROUTINE DOSTP(LABEL)
      DIMENSION LABEL(1),INS(5)
      IREAD=1
      IWRIT=1
      ITAPE=12
 4    WRITE(IWRIT,100)
 100  FORMAT("TAPE POSITION?    ")
      N=0
      READ(IREAD,101)INS
 101  FORMAT(5A2)
      IF(INS.EQ.2HRE)GO TO 1
```

```
      IF(INS.EQ.2HOK)GO TO 5
      NCHAR=IWRDS(IREAD)-4
      CALL DCODE(INS(3),NCHAR,N,IREJ)
      IF(IREJ.EQ.0)GO TO 8
      WRITE(IWRIT,105)
  105 FORMAT("ILLEGAL COMMAND")
      GO TO 4
  8   IF(INS.EQ.2HBS)GO TO 2
      IF(INS.EQ.2HFS)GO TO 3
      WRITE(IWRIT,102)
  102 FORMAT("TRY AGAIN")
      GO TO 4
  1   REWIND ITAPE
      GO TO 4
  2   CALL PTAPE(ITAPE,-N,0)
      GO TO 4
  3   CALL PTAPE(ITAPE,N,0)
      IF(IEOT(ITAPE).LT.0)GO TO 93
      GO TO 4
  5   CALL EXEC(1,114B,LABEL,37)
      IF(IEOT(ITAPE).LT.0)GO TO 93
      IF(IWRDS(ITAPE).EQ.36)GO TO 7
      WRITE(IWRIT,103)
  103 FORMAT("NO FILE NAME")
      CALL PTAPE(ITAPE,0,-1)
      GO TO 4
  7   CALL PTAPE(ITAPE,0,1)
      RETURN
  93  WRITE(IWRIT,104)
  104 FORMAT("END OF TAPE")
      GO TO 4
      END
      END$
```

```
ASMB,L
      NAM DCODE,7
      ENT DCODE
DCODE NOP
      LDB DCODE
      LDA 1,I
      STA DCODE
      INB
      LDA 1
      LDA 0,I
      RAL,CLE,SLA,ERA
      JMP *-2
      STA TADD
      INB
      LDA 1,I
      LDA 0,I
```

```
       CMA,INA
       STA CHAR
       INB
       LDA 1,I
       STA DC
       CLA
       STA DC,I
       INB
       LDA 1,I
       STA REJ
       CLA
       STA REJ,I
       LDA K5
       STA MSK
       CLB
 SAME  LDA MSK
       ALF,ALF
       STA MSK
       LDA TADD,I
       AND MSK
       SZB,RSS
       ALF,ALF
       CMB
       STA ATP
       ADA K6
       SSA,RSS
       JMP ABORT
       LDA ATP
       ADA K7
       SSA
       JMP ABORT
       STA ATP
       LDA RADIX
       ADA CHAR
       LDA 0,I
       STB BTP
       MPY ATP
       LDB BTP
       ADA DC,I
       STA DC,I
       ISZ CHAR
       RSS
       JMP DCODE,I
       CPB K8
       JMP SAME
       ISZ TADD
       JMP SAME
ABORT  CLA,INA
       STA REJ,I
       JMP DCODE,I
CHAR   BSS 1
DC     BSS 1
MSK    BSS 1
```

```
TADD  BSS 1
ATP   BSS 1
REJ   BSS 1
BTP   BSS 1
      DEC 10000
      DEC 1000
      DEC 100
      DEC 10
      DEC 1
RADIX DEF *
K5    OCT 377
K6    OCT -72
K7    OCT -60
K8    OCT -1
      END
```

```
FTN4,L
      SUBROUTINE SHADE(MX,MY,MG,LG)
C
C     THIS SUBROUTINE DRAWS A NUMBER OF DOTS IN A SPECIFIED
C     AREA OF THE SCREEN TO PRODUCE A DESIRED SHADE OF GREY.
C
C     MX,MY=POSITION OF AREA ON SCREEN
C     MG=SIZE OF AREA
C     LG=LEVEL OF GREY
C
      DIMENSION IB(2)
      COMMON IB
      ID=27040B
      IF(LG.EQ.1)GO TO 13
      IB(1)=MX
      IB(2)=MY
      CALL DOT(IB)
      IF(LG.EQ.2)GO TO 13
      IB(1)=MX+MG/2
      IB(2)=MY+MG/2
      CALL DOT(IB)
      IF(LG.EQ.3)GO TO 13
      IB(1)=MX+MG/2
      IB(2)=MY
      CALL DOT(IB)
      IB(1)=MX
      IB(2)=MY+MG/2
      CALL DOT(IB)
      IF(LG.EQ.4)GO TO 13
      DO 1 I=1,2
      DO 1 J=1,2
      IB(1)=MX+MG/4+(I-1)*MG/2
      IB(2)=MY+MG/4+(J-1)*MG/2
    1 CALL DOT(IB)
```

```
      IF(LG.EQ.5)GO TO 13
      DO 2 I=1,2
      DO 2 J=1,2
      IB(1)=MX+MG/4+(I-1)*MG/2
      IB(2)=MY+(J-1)*MG/2
    2 CALL DOT(IB)
      DO 3 I=1,2
      DO 3 J=1,2
      IB(1)=MX+(I-1)*MG/2
      IB(2)=MY+MG/4+(J-1)*MG/2
    3 CALL DOT(IB)
      IF(LG.EQ.6)GO TO 13
      DO 4 I=1,4
      DO 4 J=1,4
      IB(1)=MX+MG/8+(I-1)*MG/4
      IB(2)=MY+MG/8+(J-1)*MG/4
    4 CALL DOT(IB)
      IF(LG.EQ.7)GO TO 13
      DO 5 I=1,4
      DO 5 J=1,4
      IB(1)=MX+MG/8+(I-1)*MG/4
      IB(2)=MY+(J-1)*MG/4
    5 CALL DOT(IB)
      DO 6 I=1,4
      DO 6 J=1,4
      IB(1)=MX+(I-1)*MG/4
      IB(2)=MY+MG/8+(J-1)*MG/4
    6 CALL DOT(IB)
      IF(LG.EQ.8)GO TO 13
      DO 7 I=1,8
      DO 7 J=1,8
      IB(1)=MX+MG/16+(I-1)*MG/8
      IB(2)=MY+MG/16+(J-1)*MG/8
    7 CALL DOT(IB)
      IF(LG.EQ.9)GO TO 13
      DO 8 I=1,8
      DO 8 J=1,8
      IB(1)=MX+MG/16+(I-1)*MG/8
      IB(2)=MY+(J-1)*MG/8
    8 CALL DOT(IB)
      DO 9 I=1,8
      DO 9 J=1,8
      IB(1)=MX+(I-1)*MG/8
      IB(2)=MY+MG/16+(J-1)*MG/8
    9 CALL DOT(IB)
      IF(LG.EQ.10)GO TO 13
      DO 16 I=1,16
      DO 16 J=1,16
      IB(1)=MX+MG/32+(I-1)*MG/16
      IB(2)=MY+MG/32+(J-1)*MG/16
   16 CALL DOT(IB)
      IF(LG.EQ.11)GO TO 13
      DO 11 I=1,16
```

```
      DO 11 J=1,16
      IB(1)=MX+MG/32+(I-1)*MG/16
      IB(2)=MY+(J-1)*MG/16
   11 CALL DOT(IB)
      DO 12 I=1,16
      DO 12 J=1,16
      IB(1)=MX+(I-1)*MG/16
      IB(2)=MY+MG/32+(J-1)*MG/16
   12 CALL DOT(IB)
      IF(LG.EQ.12)GO TO 13
      DO 14 I=1,32
      DO 14 J=1,32
      IB(1)=MX+MG/64+(I-1)*MG/32
      IB(2)=MY+MG/64+(J-1)*MG/32
   14 CALL DOT(IB)
      IF(LG.EQ.13)GO TO 13
      DO 15 I=1,32
      DO 15 J=1,32
      IB(1)=MX+MG/64+(I-1)*MG/32
      IB(2)=MY+(J-1)*MG/32
   15 CALL DOT(IB)
      DO 17 I=1,32
      DO 17 J=1,32
      IB(1)=MX+(I-1)*MG/32
      IB(2)=MY+MG/64+(J-1)*MG/32
   17 CALL DOT(IB)
      IF(LG.GT.16)GO TO 10
   10 WRITE(1,100)
  100 FORMAT("TOO MANY GREY LEVELS")
   13 RETURN
      END
      END$
```

```
FTN4,L
      SUBROUTINE DOT(IB)
C
C     THIS SUBROUTINE WRITES A PERIOD (.) AT THE SCREEN
C     POSITION STORED IN "IB".
C
      DIMENSION IB(2)
      ID=27040B
      CALL EXEC(2,3001B,IB,1)
      CALL EXEC(2,0001B,ID,1)
      RETURN
      END
      END$
```

```
FTN4,L
      SUBROUTINE BOX(MX,MY,IT)
C
C     THIS SUBROUTINE DRAWS A BOX AND PRODUCES A SCALE
C     ALONG ITS EDGES
C
C     MX,MY=MAXIMUM VALUES OF X,Y SCALES
C     "IT" DETERMINES WHETHER SCALE IS IN MM. OR
C     CHANNEL NUMBERS
C
      DIMENSION ICORN(2,5),IDIGT(2)
C
      EQUIVALENCE(ICORN,IDIGT)
C
C     DRAW BOX
      ICORN(1,1)=255
      ICORN(2,1)=133
      ICORN(1,2)=255+512
      ICORN(2,2)=133
      ICORN(1,3)=255+512
      ICORN(2,3)=133+512
      ICORN(1,4)=255
      ICORN(2,4)=133+512
      ICORN(1,5)=255
      ICORN(2,5)=133
      CALL EXEC(2,3001B,ICORN,5)
C
C     DRAW NINE MARKERS ALONG EACH SIDE
      DO 6 I=1,9
      ICORN(1,1)=255+(I-1)*64
      ICORN(2,1)=645+5
      ICORN(1,2)=ICORN(1,1)
      ICORN(2,2)=645-5
      CALL EXEC(2,3001B,ICORN,2)
      ICORN(2,1)=133+5
      ICORN(2,2)=133-5
    6 CALL EXEC(2,3001B,ICORN,2)
      DO 7 I=1,9
      ICORN(1,1)=255-5
      ICORN(2,1)=133+(I-1)*64
      ICORN(1,2)=255+5
      ICORN(2,2)=ICORN(2,1)
      CALL EXEC(2,3001B,ICORN,2)
      ICORN(1,1)=767-5
      ICORN(1,2)=767+5
    7 CALL EXEC(2,3001B,ICORN,2)
C
C     DRAW SCALE ALONG EDGES
      DO 2 I=0,8
      NUMB=I*MX/8
      IDIGT(1)=256+64*I-30
      IDIGT(2)=134-35
C
```

```
C       DRAW SCALES ALONG EDGES
        CALL EXEC(2,3001B,IDIGT,1)
      2 WRITE(1,100)NUMB
    100 FORMAT(I3)
        DO 3 J=0,8
        NUMB=J*MY/8
        IDIGT(1)=256-60
        IDIGT(2)=134+64*J-8
        CALL EXEC(2,3001B,IDIGT,1)
      3 WRITE(1,100)NUMB
        IDIGT(1)=0
        IDIGT(2)=390
        CALL EXEC(2,3001B,IDIGT,1)
        IF(IT.EQ.0)GO TO 4
C
C       IF IT=1, WRITE "MM" BESIDE SCALE
        WRITE(1,101)
    101 FORMAT("MM")
      4 RETURN
        END
        END$
```